Hepatitis C virus (HCV) is a single-strand, positive-sense RNA virus belonging to the flaviviridae family. HCV develops persistent infection in <70% of infected patients, and eventually causes chronic hepatitis, cirrhosis, and hepatocellular carcinoma in some patients.[1] Once chronic infection is established in patients with HCV, spontaneous viral clearance fails,[1] although how HCV remains persistently infecting the liver is unknown. It has been accepted that successful viral clearance by the host is largely attributed to robust induction of type I interferon (IFN) and antiviral cellular effectors, cytotoxic T lymphocyte (CTL) and natural killer (NK) cells.[2-5] In HCV-infected patients and chimpanzees, type I IFN induction and activation of HCV-specific $CD4^+$ T/$CD8^+$ T cells and NK cells are indeed detected during acute infection.[4-6] However, why these antiviral factors cannot eradicate HCV from most patients is not addressed. Facilities for inducing the antiviral effectors and their role against HCV persistence have not been well determined. A main cause for the deficiency of knowledge on the host response to HCV is the lack of an appropriate model for experimental HCV infection.

Two breakthroughs have now made it possible to investigate the immune response against HCV. First, Toll-like receptors (TLRs) and other innate immune receptors of dendritic cells (DCs) were found to be involved in the host antiviral IFN response, followed by CTL and NK cell activation.[2,7-9] Some reports revealed that HCV proteins participate in the regulation of IFN-inducing innate responses.[10-12] Second, an *in vitro* amplifiable 2a type HCV strain, JFH1, was established by Wakita et al.[13] and Zhong et al.[14] Infection studies for testing HCV replication and the immune response are therefore now feasible *in vitro*.

There are two major subsets of DCs in humans: plasmacytoid DCs (pDCs) expressing TLR7 and TLR9 and myeloid DCs expressing Toll-like receptor 3 (TLR3) for viral RNA/DNA recognition. Cytoplasmic RNA sensors, retinoic acid inducible gene I (RIG-I)-like receptors, also participate in viral RNA recognition and IFN induction.[7] RNA virus infection allows pDCs to induce type I IFN via TLR7.[15] On the contrary, myeloid DCs recognize virus-derived double-stranded RNA (dsRNA) to activate pathways for IFN-beta production and NK/CTL induction.[7-9,16] What happens in the pathway of myeloid DC maturation during HCV infection can now be experimentally followed up in infected cells as the JFH1 strain can be used for *in vitro* infection studies. Hence, we inoculated monocyte-derived (Mo)DCs with JFH1 of HCV.

Here, we show evidence that the JFH1 strain has no direct route for MoDC infection and MoDCs phagocytosing HCV-infected apoptotic vesicles participate in MoDC maturation and reciprocal activation of T cells and NK cells.

Materials and Methods

Cell Lines, Antibodies, and Reagents. Huh7.5.1 cells were kindly provided by Dr. Francis V. Chisari (The Scripps Research Institute, La Jolla, CA), and maintained in Dulbecco's modified Eagle's medium–based medium.[14] Following materials were obtained as indicated: anti-HCV-core monoclonal antibody (mAb; C7-50) from Affinity BioReagents (Golden, CO), mAbs against CD80, CD83, and CD86 from Immunotech (Fullerton, CA), anti-dsRNA mAb (K1) from English & Scientific Consulting Bt (Szirak, Hungary), biotin-conjugated anti-TLR3 mAb from eBioscience (San Diego, CA), fluorescein isothiocyanate–labeled goat anti-mouse immunoglobulin G from American Qualex (San Clemente, CA), Streptavidin Alexa Fluor 594 conjugate and SNARF1 from Molecular Probe (Carlsbad, CA), Methyl-beta-cyclodextrin (MβCD), chlorpromazine (CPZ), and bafilomycin (BAF) from Sigma-Aldrich (St. Louis, MO).

Preparation of Immature MoDCs, NK Cells, and T Cells. $CD14^+$ monocytes and autologous NK cells were isolated from human peripheral blood mononuclear cells (PBMCs) using a MACS system (Miltenyi Biotec, Bergisch Gladbach, Germany).[17] Cells purified by this technique had an average purity of 95%, as assessed by flow cytometry. Immature MoDCs were generated from monocytes using human granulocyte-macrophage colony-stimulating factor (GM-CSF; PeproTech, Rocky Hill, NJ) and interleukin (IL)-4 (PeproTech).[17] Autologous NK cells were stocked in Cell Banker (Diaton, Tokyo, Japan) at −80°C. Allogeneic $CD4^+$ and $CD8^+$ T cells were also negatively isolated by a MACS system (Miltenyi Biotec).

Stimulation of Immature MoDC, Cytokine Assay, Immunofluorescent Staining, and Flow Cytometry. The immature MoDCs (2×10^5) were inoculated with HCV and respiratory syncytial virus (RSV) at a multiplicity of infection (MOI) of one or treated with polyinosinic: polycytidylic acid (poly I:C; 10 μg/mL), and cultured in a 24-well plate. The cells and culture supernatant were harvested at indicated time points for reverse transcription polymerase chain reaction (RT-PCR), fluorescence-activated cell sorting (FACS), and enzyme-linked immunosorbent assay (ELISA; IFN-beta, IFN-gamma; Fujirebio, Inc., Tokyo, Japan; IL-6; BD Biosciences, Franklin Lakes, NJ). In some experiments, immature MoDCs (2×10^5) were cocultured with HCV- or non-infected apoptotic cells (4×10^5). MoDCs were treated with MβCD (1 mM), CPZ (5 μg/mL), and BAF (100

nM) for 1 hour before coculture. The viability of these MoDCs was examined by proidium iodide staining. After 2 days of coculture, the MoDCs were isolated from the apoptotic cells by Ficoll-Paque Plus (GE-Healthcare, Waukesha, WI) using the manufacturer's methods, and used for further analysis to assess MoDC functions. The cell lysates were produced from the apoptotic cells by three freeze/thaw cycles, followed by centrifugation at 15,000 rpm for 5 minutes or by sonication three times for 20 seconds on ice. Total RNA was extracted by Trizol (Invitrogen, Carlsbad, CA) by the manufacturer's methods. MoDCs (5×10^5 cells) were transfected with 0.625 μg total RNA by N-[1-(2,3-Dioleoyloxy)propyl]-N, N, N-trimethylammonium methyl-sulfate (DOTAP; Roche, Mannheim, Germany) and cultured in 24-well plates for 1 day. Huh7.5.1 cells were transfected with poly I:C using Lipofectamine 2000 (Invitrogen) by the manufacturer's methods. ELISA for determination of cytokine levels, flow cytometry, and immunofluorescent staining were performed as reported.[17,18]

Virus Propagation. The method to generate infectious HCV particles was referred to an *in vitro* system using the plasmid pJFH-1.[16] Noninfected cell supernatant was used as noninfected control. The concentrated virus had a titer of 1 to 2×10^6 ffu/mL. A RSV field-isolate strain (RSV2177) was propagated with Hep-2 cells as described.[17] The titer of RSV2177 was determined by 50% tissue culture infective dose (TCID50) with Hep-2 cells.

Real-time PCR Quantification of Positive-Strand and Negative-Strand HCV RNA. Total Trizol-extracted RNA was analyzed by reverse transcription-PCR (RT-PCR) with a modification of the previously described strand-specific rTth RT-PCR method.[19] RT primers for complementary DNA synthesis of positive and negative strand HCV RNA were GTGCACGGTCTACGAGACCT and GAGTGTCGTACAGCCTCCAG, respectively. Positive-strand and negative-strand HCV PCR amplifications were performed using Platinum SYBR Green qPCR SuperMix-UDG (Invitrogen) with 200 nM of paired primers, forward CGGGAGAGCCATAGTGG and reverse AGTACCACAAGGCCTTTCG. The PCR conditions were 95°C for 10 minutes, followed by 40 cycles of 95°C for 15 seconds and 60°C for 1 minute. This PCR method could detect 10 copies of positive-strand or negative-strand HCV.

Induction and Certification of Apoptosis. A total of 1×10^5 Huh7.5.1 cells were plated in a 24-well plate and infected with the JFH1 strain at an MOI of 1. At indicated timed intervals, the infected cells and poly I:C-transfected cells were pretreated with cycloheximide

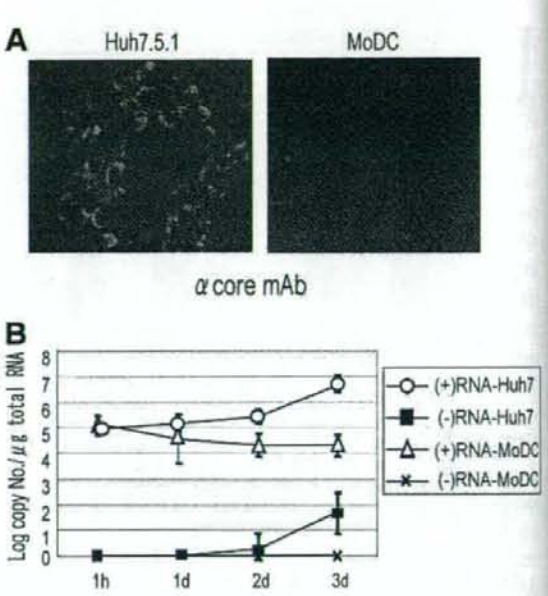

Fig. 1. MoDCs are not permissive for HCV replication. (A) Huh7.5.1 cells and MoDCs were inoculated with HCV at an MOI of 1 and cultured for 3 days. The presence of HCV core antigens was assessed by immunofluorescent staining. (B) Real-time RT-PCR to detect positive-strand and negative-strand HCV RNA. Data show means ± SD from three independent experiments using three different donors.

(20 μg/mL; Sigma) for 30 minutes, followed by tumor necrosis factor (TNF)-alpha (10 ng/mL; Pepro-Tech). The HCV-infected and noninfected apoptotic cells were harvested after another 24-hour culture. Using the HCV-infected apoptotic cells, we examined the presence of HCV core antigens and dsRNA by FACS using anti-HCV core mAb and anti-dsRNA mAb, respectively. Apoptosis was assessed by 4',6-diamidino-2-phenylindole-staining, DNA fragmentation, and FACS by using fluorescein isothiocyanate–labeled annexin-V and proidium iodide (Roche).[20]

Assay for Lymphocyte Proliferation by MoDC. After 2 days culture of MoDCs with HCV, poly I:C (10 μg/mL), or the apoptotic cells, MoDCs were harvested and treated with mitomycin C (20 μg/mL) in phosphate buffered saline for 45 minutes. For the proliferation assay, the stimulated-MoDCs (1×10^4) were cultured with 1×10^5 allogeneic PBMCs, $CD4^+$ T cells, or $CD8^+$ T cells in U-bottom 96-well plates for 6 days. During the last 24 hours of culturing, [^{3}H]thymidine (1 mCi/well) was added to the culture medium. Then the cells and medium were harvested separately by a cell-harvester, and the radioactivity was measured by a liquid scintillation counter (Aloca, Tokyo, Japan). For the analysis of $CD4^+$ T cell polarization, the stimulated-MoDCs (1×10^4) were

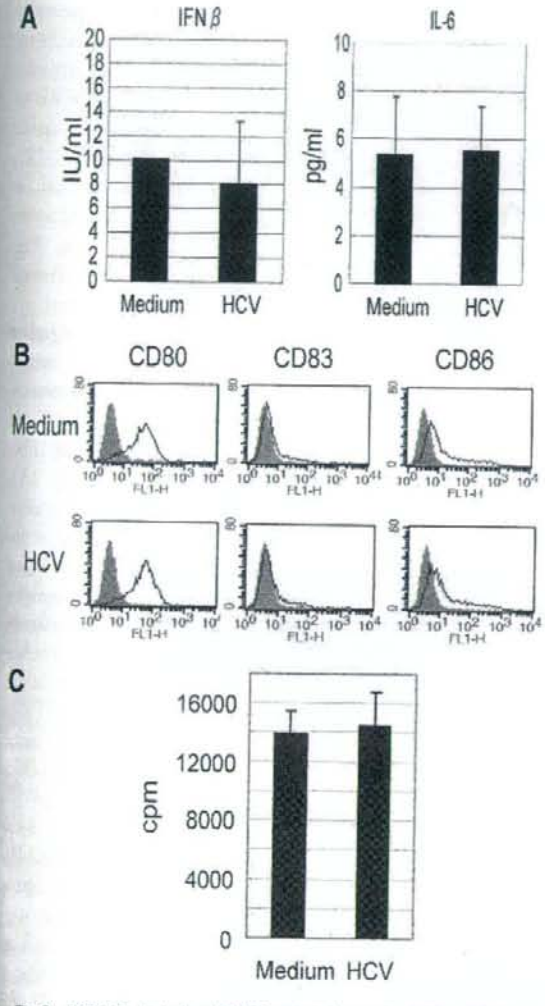

Fig. 2. HCV fails to induce MoDC maturation and cytokine response. MoDCs were inoculated with HCV at an MOI of 1 and cultured for 48 hours. (A) The supernatant was assayed for production of IFN-beta and IL-6. (B) The cells were harvested for FACS and (C) mixed lymphocyte reaction (MIR). Allogeneic PBMC were cultured with the inoculated-MoDCs for 6 days. Proliferation was determined by [^{3}H]thymidine uptake. Data show means ± SD of duplicate or triplicate samples from one experiment representative of three donors.

treated with mitomycin C and cultured with allogeneic CD4$^+$ T cells (1×10^5) for 6 days. Then the cells were washed and transferred to new round-bottom 96-well plates. Phorbol 12-myristate 13-acetate (10 ng/mL; Sigma-Aldrich) and ionomycin (1 μg/mL; Sigma-Aldrich) were added and plates were incubated for a further 24 hours. Supernatants were harvested for cytokine production (IL-4, IFN-gamma; GE-Healthcare).

MoDC-NK Coculture and ^{51}Cr Release Assay. The stimulated-MoDCs were harvested for MoDC-NK coculture at indicated time points. Autologous NK cells (5×10^5) were cocultured with the MoDCs (1×10^5) in 24-well plates for 24 hours. Transwell (Corning) was inserted to block the MoDC-NK cell contact. The supernatants and NK cells were collected from the MoDC-NK coculture and assayed for IFN-gamma production (GE Healthcare) and cytotoxicity against K562. Cytotoxicity was determined by standard ^{51}Cr release assay as described.[17]

Gene Silencing of TLR3 in MoDC. Small interfering RNA (siRNA)-based gene knockdown was preformed with MoDCs by electroporation as described.[21] siRNA duplexes (small interfering TLR3: cat #107056, negative control: cat #AM4635) were obtained from Ambion (Tokyo, Japan). Expression of TLR3 was examined by SYBR green real-time PCR using forward primer, AAGACCCATTATG-CAAAAGATTCAA and reverse primer, TCCAGATTTT-GTTCAATAGCTTGTTG. MoDCs (1×10^6 cells) were electroporated with these siRNA and cultured for 4 hours. Then, HCV-infected or noninfected apoptotic Huh7.5.1

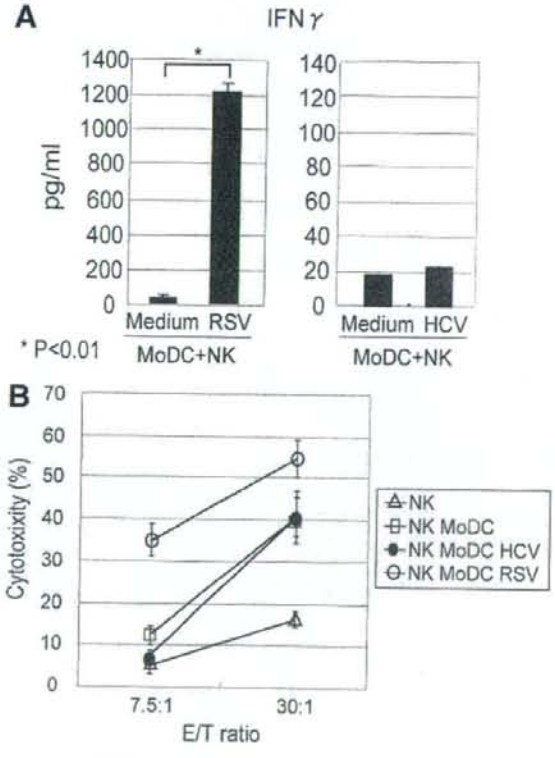

Fig. 3. MoDCs inoculated with HCV barely activate NK cells. MoDCs were harvested at 24 hours after inoculation of RSV and HCV. Autologous NK cells were cocultured with the MoDCs for 24 hours. (A) The supernatant were assayed for NK IFN-gamma production. (B) NK cells were harvested for ^{51}Cr release assay to examine NK cytotoxic activity against K562. A representative of the three similar experiments with individual donors is shown.

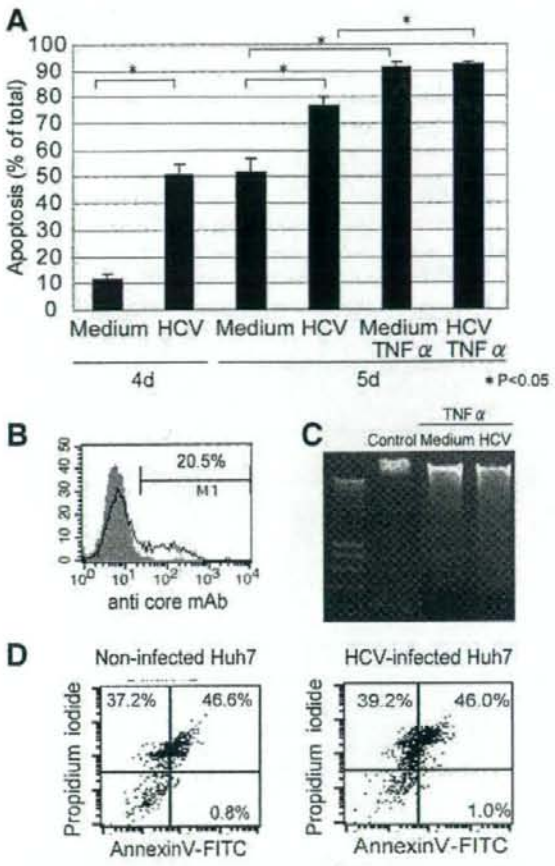

Fig. 4. Preparation of HCV-infected apoptotic Huh7.5.1 cells. Huh7.5.1 cells were infected with HCV at an MOI of 1 and culture for 4 or 5 days. Apoptosis was induced by cycloheximide and TNF-alpha after 4 days culture. At 5 days after infection, the apoptotic cells were harvested for counting 4',6-diamidino-2-phenylindole stained apoptotic nuclei, FACS and examination of DNA fragmentation. (A) Typical apoptotic cells stained with 4',6-diamidino-2-phenylindole were counted among <1000 cells and percent cell apoptosis was determined. Data are means ± SD from three independent experiments, each performed in triplicate. (B) HCV-core antigens were detected in the HCV-infected apoptotic cells by FACS. (C) DNA was extracted from HCV- or noninfected apoptotic Huh7.5.1 cells and electrophoresed on agarose gels to evaluate DNA fragmentation. (D) HCV- and noninfected Huh7.5.1 cells were examined for stages of apoptosis by FACS using annexin V-fluorescein isothiocyanate (FITC) and proidium iodide. Data shown are representative of three independent experiments.

cells (2×10^6 cells) were added to the wells. After 48 hours of culture, the supernatants were harvested and examined for cytokine concentrations by ELISA.

Results

MoDCs Are Not Permissive for HCV Replication. MoDCs and Huh7.5.1 cells were inoculated with the JFH1 strain at an MOI of 1, then the cells were harvested for immunofluorescent staining and sequence-specific real-time RT-PCR at indicated time points after inoculation. HCV genome RNA (negative sense of HCV RNA) was replicated in Huh7.5.1 cells but not to a detectable level in MoDCs at 2 to 3 days after inoculation (Fig. 1B). Accordingly, HCV core antigens were detected in Huh7.5.1 cells, but not in MoDCs, by immunofluorescent staining until 3 days after HCV inoculation (Fig. 1A). Similar results were obtained with monocyte-derived macrophages and BDCA4$^+$ pDCs (data not shown).

MoDC Maturation and Cytokine Response Against the JFH1 Strain. DCs work as key producers of innate inflammatory cytokines in response to pathogen-associated molecular patterns (PAMPs). However, MoDCs inoculated with JFH1 (MOI = 1) did not produce IFN-gamma or IL-6 over the noninfected control (Fig. 2A). MoDCs stimulated with PAMPs mature to up-regulate CD80/CD86 expression and activate T cells. Some reports showed that the MoDC maturation was induced following incorporation of HCV pseudotype particles into the MoDCs.[22] However, expression of costimulatory molecules (CD80, CD86) and a maturation marker (CD83) were not up-regulated by inoculation with the JFH1 strain (MOI = 1; Fig. 2B). MoDCs cocultured with JFH1 strain did not enhance the proliferation of allogeneic PBMC compared with noninoculated MoDCs (Fig. 2C).

MoDCs Exposed to the JFH1 Strain Do Not Activate NK Cells. MoDCs are known to recognize PAMPs and promote NK cell activation via MoDC/NK reciprocal interaction.[9] We have reported that NK cells are activated by MoDCs infected with RNA viruses, such as RSV, influenza virus, and measles virus.[17] We inoculated MoDCs with RSV or the JFH1 strain at an MOI of 1 and cocultured the MoDCs with autologous NK cells. After 1-day of coculture, NK cell IFN-gamma and cytotoxicity were markedly induced by RSV-treated MoDCs but not HCV-treated MoDCs (Fig. 3A,B).

HCV-Infected Apoptotic Cells Induce MoDC Maturation and Cytokine Responses. Then, we moved on to whether HCV-infected cells affect MoDC maturation. We first cocultured MoDCs with HCV-infected or noninfected Huh7.5.1 cells and examined IL-6 production by MoDCs. MoDCs cocultured with HCV-infected Huh7.5.1 cells secreted more IL-6 than those with noninfected Huh7 cells (Fig. 5A). However, since HCV infection induced apoptosis in Huh7.5.1 cells, HCV-infected and noninfected Huh7 cells were not in the same apoptotic stages (Fig. 4A). We had to exclude the possibility that apoptotic events themselves affect MoDC maturation. Therefore, we forced HCV-infected and

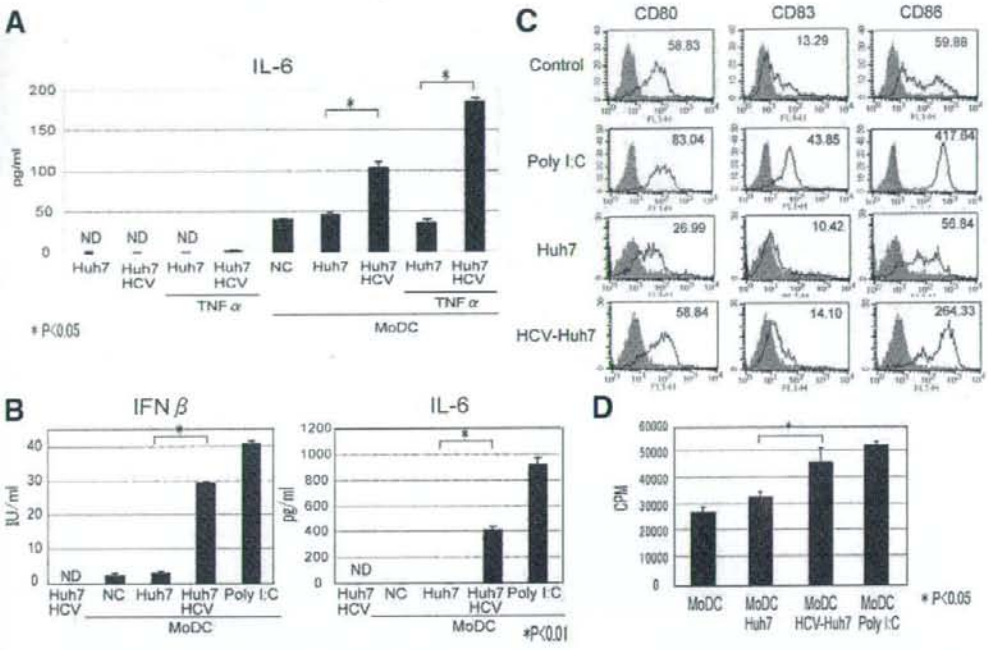

Fig. 5. HCV-infected apoptotic cells induce MoDC maturation and cytokine response. MoDCs were cocultured with HCV-infected/noninfected apoptotic or nonapoptotic cells for 2 days. Polyl:C stimulation was used as a positive control. (A,B) The culture supernatants were assayed for determination of IFN-beta and IL-6. The MoDCs were isolated from the apoptotic cells and used for (C) FACS and (D) mixed lymphocyte reaction (MLR). MoDC maturation was examined by the expression of CD80, CD83, and CD86 (C, a representative of three donor experiments). Allogeneic PBMCs were cultured with the MoDCs for 6 days. Proliferation was determined by [^{3}H]thymidine uptake (D, means ± SD of triplicate samples from one representative of three donors).

noninfected cells to induce full apoptosis by cycloheximide and TNF-alpha to the same level of apoptotic stages (Fig. 4A). HCV core antigens were detected in 20.5% of the HCV-infected apoptotic cells (Fig. 4B). Apoptotic nuclei were observed in almost all of HCV-infected and noninfected cells (Fig. 4A). DNA ladder formation, a hallmark of apoptosis, was detected in HCV-infected and noninfected apoptotic Huh7.5.1 cells to similar levels (Fig. 4C). Apoptotic cells, either infected or noninfected, gave similar profiles by flow cytometry using annexin-V for early apoptosis and propidium iodide for late apoptosis (Fig. 4D).

We applied these HCV-infected and noninfected apoptotic cells to MoDCs and determined the concentration of IFN-beta and IL-6 in the culture supernatants. HCV-infected apoptotic cells facilitated the production of IFN-beta and IL-6 by MoDCs compared with noninfected apoptotic cells (Fig. 5B). In this context, HCV products, rather than undergoing apoptosis, in infected cells are an essential factor for induction of MoDC maturation (Fig. 5A).

We next examined whether MoDC maturation was induced by HCV-infected apoptotic cells. After coculture of MoDCs with the apoptotic cells, MoDCs were isolated from the apoptotic cells using Ficol Paque. Purity of these isolated MoDCs reached over 98%, judged by 5(6)-Carboxyfluorescein diacetate N-succinimidyl ester labeled MoDCs (data not shown). CD86 of the maturation markers on MoDCs (Fig. 5C) was especially more expressed on these cells by HCV-infected apoptotic cells than by noninfected apoptotic cells. HCV-infected apoptotic cells slightly enhanced the expression levels of major histocompatibility complex class I, class II, and human leukocyte antigen-E on MoDCs (data not shown). MoDCs also acquired the increased ability to stimulate allogeneic PBMCs, $CD4^+$ T cells, and $CD8^+$ T cells in response to HCV-infected apoptotic cells (Figs. 5D and 6A).

We determined the ability of $CD4^+$ T cells to produce IFN-gamma (a Th1 cytokine) and IL-4 (a T helper 2 cytokine) after coculture of allogeneic $CD4^+$ T cells and MoDCs exposed to HCV-infected apoptotic cells. These $CD4^+$ T cells produced higher levels of IFN-gamma and lower levels of IL-4 (Fig. 6B) compared to the noninfected control, suggesting that HCV-infected apoptotic cells modulate MoDC func-

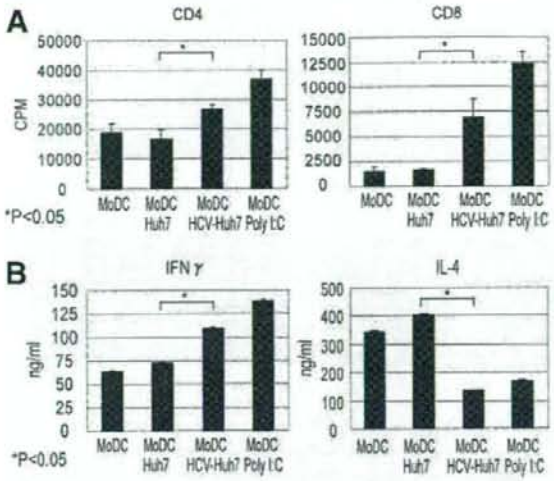

Fig. 6. HCV-infected apoptotic cells modulate MoDC function to polarize the Th1 shift. (A) After 2 days culture with HCV-infected and noninfected apoptotic cells, the isolated MoDCs (1×10^4) were cultured with allogeneic $CD4^+$ T cells and $CD8^+$ T cells (1×10^5) for 6 days. Proliferation was determined by [^{3}H]thymidine uptake. (B) Allogeneic $CD4^+$ T cells were harvested after 6 days culture with the MoDCs and stimulated with phorbol 12-myristate 13-acetate and ionomycin for 24 hours. The supernatants were collected to assess the levels of IFN-gamma and IL-4 by ELISA. Poly I:C stimulation was used as a positive control. Data shown are means ± SD of duplicate or triplicate samples from one experiment representative of three donors.

tion to promote Th1-dominant immunity in the Th1/T helper 2 balance.

HCV-Infected Apoptotic Cells Stimulate MoDCs To Activate NK Cells. We next evaluated whether these mature MoDCs could enhance NK activity via MoDC-NK interaction. After exposure of MoDCs to HCV-infected or noninfected apoptotic cells, MoDCs were isolated as described above. HCV-infected apoptotic cells promoted MoDC function to augment NK cell cytotoxicity but not IFN-gamma production compared to noninfected cells (Fig. 7A,B). This up-regulation of NK cell cytotoxicity through MoDC-NK interaction was canceled by separating MoDCs from NK cells with a transwell insertion (Fig. 7C). This suggested that cell-cell contact was the key factor for MoDC-mediated NK cell cytotoxicity induced by coculture with HCV-infected apoptotic cells.

MoDC Maturation Relied on TLR3 Signal Evoked by dsRNA in Apoptotic Vesicles. We surveyed the mechanism of MoDC maturation by HCV-infected apoptotic cells. Since HCV is a positive single-strand RNA virus, dsRNA was detected in HCV-containing apoptotic vesicles by mAb against dsRNA (Fig. 8A). To investigate whether MoDCs were taking up these apoptotic vesicles, we labeled HCV-infected apoptotic cells with the far red fluorescent dye, SNARF-1. MoDCs phagocytosed the SNARF-1-labeled vesicles containing dsRNA, which partially colocalized with TLR3 (Fig. 8B,C). N-[1-(2,3-Dioleoyloxy)propyl]-N, N, N-trimethylammonium methylsulfate (DOTAP)-based transfection was employed for the targeting of RNA to the TLR3-containing endosome.[23] HCV-derived RNA allowed MoDCs to induce IL-6 production as in control poly I:C (Fig. 8D). IL-6 of

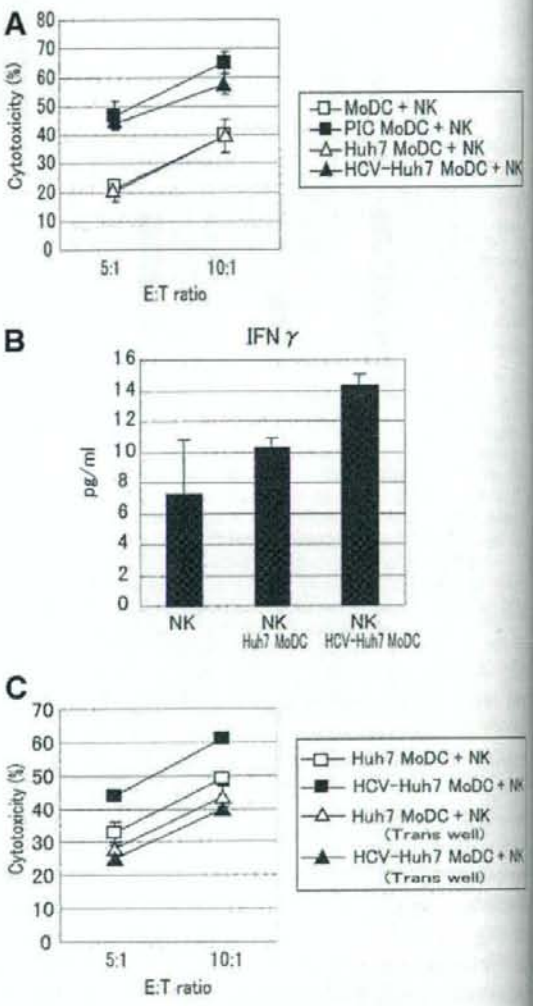

Fig. 7. NK cell activation by MoDCs exposed to HCV-infected apoptotic cells. After 2 days culture with HCV-infected and noninfected apoptotic cells, the isolated MoDCs were cultured with autologous NK cells for 24 hours. (A) NK cytotoxic activity against K562 was determined by ^{51}Cr release assay. Poly I:C stimulation was used as positive control. (B) Supernatant of the MoDC-NK coculture was assayed for NK cell IFN-gamma production. In some experiments, transwell was used to block MoDC-NK cell contact. (C) Using these NK cells, cytotoxic activity was measured by ^{51}Cr release assay. Data shown are means ± SD of duplicate or triplicate samples from one experiment representative of three donors.

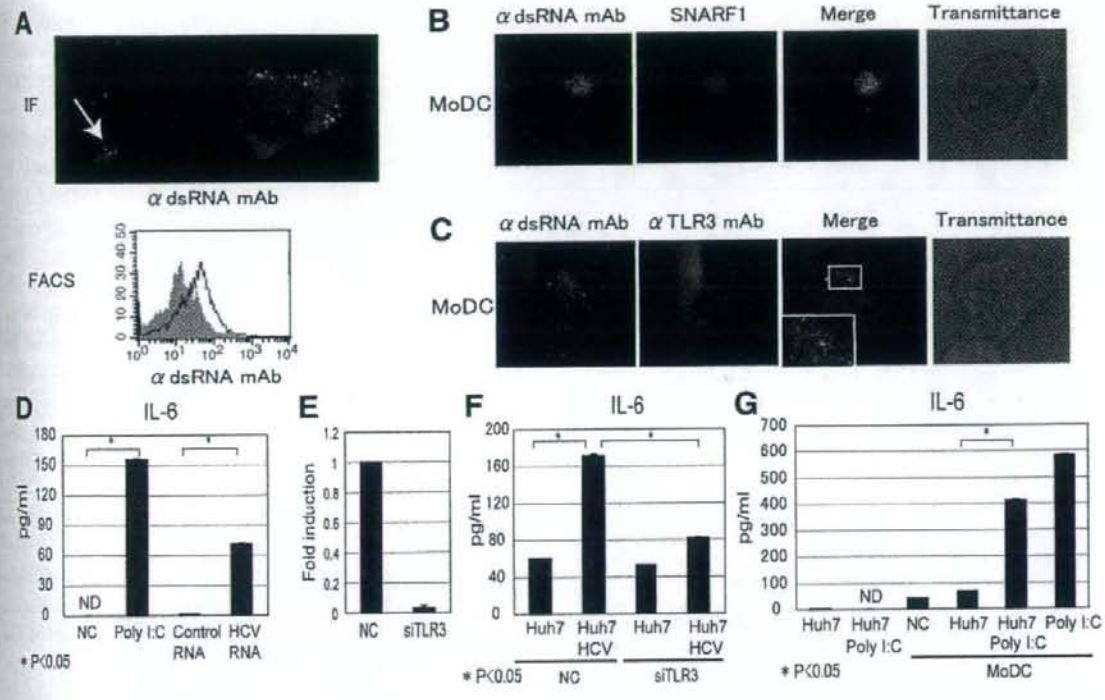

Fig. 8. TLR3 signaling by dsRNA contained in apoptotic vesicles induces MoDC maturation. (A) HCV-infected apoptotic Huh7.5.1 cells were labeled with SNARF1. dsRNA was detected in HCV-infected apoptotic cells and vesicles (arrow) by immunofluorescent assay (upper panel) and FACS using anti-dsRNA mAb (lower panel). (B,C) MoDCs were exposed to HCV-infected apoptotic cells for 4 hours and harvested for immunofluorescent assay. The MoDCs were isolated with Ficoll-Paque and stained with mAbs against dsRNA or human TLR3. (D) MoDCs were transfected with total RNA extracted from HCV-infected or noninfected Huh7.5.1 cells. After 1 day of culture, the levels of IL-6 were determined. Poly I:C was positive control. (E) The level of TLR3 messenger RNA (mRNA) was determined 1 day after siRNA electroporation. (F) Knockdown of TLR3 partially abolishes the IL-6 production by MoDCs. Data shown are means ± SD of duplicate or triplicate samples from one experiment representative of three donors. (G) Poly I:C-transfected apoptotic Huh7.5.1 cells induced MoDCs to produce IL-6.

inflammatory cytokine was a representative marker for TLR3 signal in this case, suggesting that at least HCV RNA, rather than proteins, participates in MoDC maturation.

Since siRNA knockdown of TLR3 in MoDCs was successfully executed by electroporation of MoDCs with TLR3-targeted siRNA (Fig. 8E), we tested whether the level of IL-6 was affected in the TLR3-depleted MoDCs stimulated with apoptotic vesicles containing dsRNA of HCV propagation. TLR3-depleted MoDCs retarded maturation into decreased IL-6 production (Fig. 8F). Poly I:C-transfected Huh7.5.1 apoptotic cells stimulate MoDCs to secret IL-6 (Fig. 8G). Taken together, phagocytosed HCV-infected apoptotic cells can provoke TLR3 signaling in MoDCs, which participates in MoDC maturation.

MoDCs are known to take up polyI:C, a synthetic dsRNA, which is recognized by TLR3. Therefore, MoDC maturation may be elicited by direct MoDC uptake of dsRNA produced during HCV replication. However, CD86 up-regulation was not observed on MoDCs stimulated with freeze/thaw cell lysates and sonicated apoptotic cells from HCV-infected Huh7.5.1 cells (Fig. 9A). For MoDC maturation, dsRNA was required to be wrapped in vesicles.

We next treated MoDCs with CPZ (a known inhibitor of clathrin-mediated endocytosis), BAF (a specific inhibitor of the vacuolar H^+-adenosine triphosphatase), and methyl-beta-cyclodextrin (MβCD, which depletes or sequesters membrane cholesterol, inhibiting endocytic pathways dependent on lipid rafts) to evaluate the possible involvement of endocytosis in MoDC maturation. MβCD had an inhibitory effect on MoDC maturation (Fig. 9B) and cytokine responses (data not shown) by HCV-infected apoptotic cells. Lipid rafts appeared to play some important roles in the uptake of HCV-infected apoptotic cells.

Discussion

MoDC recognizes pattern molecules of pathogen to signal the presence of microbial infection.[7] Pattern recog-

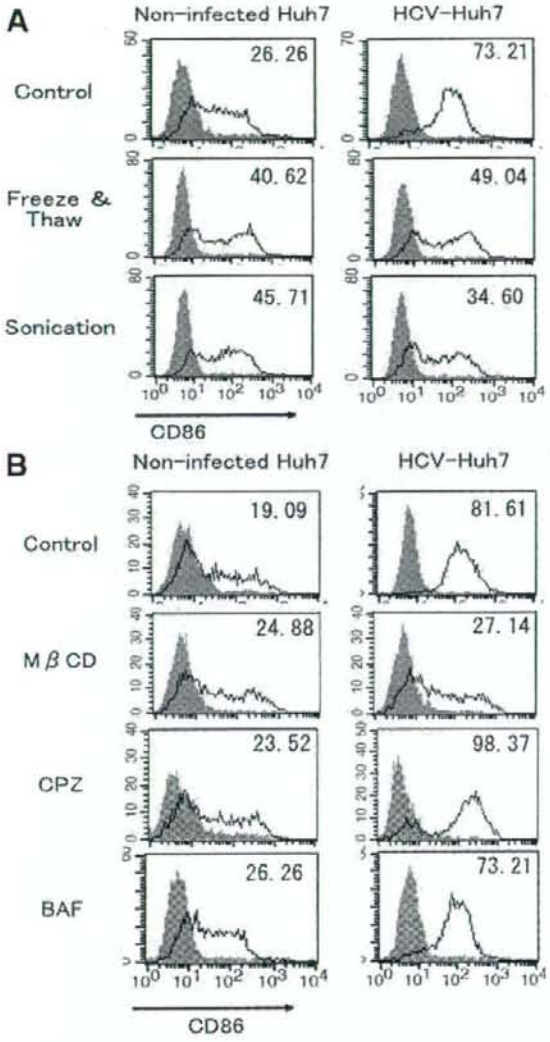

Fig. 9. Lipid raft-dependent phagocytosis of dsRNA-including apoptotic vesicles is required for MoDC maturation. (A) HCV-infected or noninfected apoptotic cells were prepared as described. The expression of CD86 was examined on MoDCs stimulated with apoptotic cell lysates prepared by freeze-thaw or sonication. (B) MoDCs were treated with methyl-beta-cyclodextrin (MβCD), CPZ, and BAF for 1 hour, followed by coculture with HCV-infected or noninfected apoptotic cells for 2 days. The MoDC CD86 expression was determined by FACS. Data from a representative of three donors are shown.

nition and antigen uptake are two central events in the activation of cellular immunity. How HCV infection elicits MoDC maturation and NK activation is the theme of this study. The following results were obtained with the JFH1 HCV strain and human MoDC. MoDCs mature via phagocytosing infected hepatocytes, but not through direct infection. MoDCs taking up HCV-infected apoptotic vesicles containing dsRNA activate T cells and NK cells. The mature MoDCs also polarized $CD4^+$ T cells into the Th1 type. Thus, HCV-infected apoptotic hepatocytes are a source of HCV antigen and PAMPs.

These *in vitro* results cast light on the mechanism of CTL and NK cell activation against HCV in patients. In the liver of patients, immature human MoDCs may phagocytose bystander hepatocytes when the cells undergo apoptosis secondary to HCV infection. The MoDCs that incorporate HCV-infected vesicles into the phagosomes are able to secrete cytokines including IFN-beta and IL-6. These MoDC responses are enabled by fusing HCV-derived dsRNA with phagosomal TLR3. Activation of the MoDC TLR3 pathway, as has been reported,[8,16] have a crucial role in development of the MoDC TLR3-mediated NK activation and CTL induction.

MoDCs express endogenous DC-SIGN, which captures pseudotype lentivirus particles expressing HCV glycoproteins E1 and E2 and may transmit HCV particles to adjacent hepatocytes.[24] Pseudotype vesicular stomatitis virus coated with chimeric E1 and E2 enters MoDCs through interaction with lectins.[22] These pseudotype HCV studies suggested that MoDCs capture, and in some cases internalize, HCV particles only when expressing E1/E2. In fact, many candidates of the HCV entry receptor have been reported and MoDCs express CD81, scavenger receptor class B type I, and DC-SIGN.[24,25] However, the actual ligand-receptor interaction in HCV MoDC infection has not been demonstrated even in CD81 and DC-SIGN. Our results suggest that phagocytosis of HCV-infected apoptotic cells, but not direct interaction between MoDCs and HCV particles, serves as an inducer of MoDC maturation. The molecules on HCV-infected cells rather than those only in the virion may participate in induction of MoDC-mediated HCV cellular immunity.

NK cells play a role to prevent persistent HCV infection. An epidemiologic survey showed that genes encoding the weak inhibitory NK cell receptor KIR2DL3 and its human leukocyte antigen C group1 ligand are directly associated with HCV eradication in patients.[3] Since the cell-cell contact is indispensable for MoDC-mediated NK activation, soluble factors such as type I IFN and IL-15 may only have a peripheral role in the emergence of HCV-derived NK cells. We have shown that natural killer group 2, member D (NKG2D) ligands on MoDCs which interact with NKG2D on NK cells are involved in MoDC-mediated NK cell activation against RNA virus infection and poly I:C.[9] The NKG2D/NKG2D ligand interaction was partially responsible for NK activation by MoDCs after uptake of dsRNA-containing vesicles (data

not shown). Yet the main ligand for NK activation on MoDCs is still undetermined. Searching for dsRNA-inducible NK activation ligands in MoDCs would foster identification of MoDC factors reciprocally activating NK cells.

In general, high replication of viruses results in cell death by apoptosis and necrosis. Our study on HCV suggests that apoptotic alteration occurs in HCV-infected Huh7.5.1 cells. These HCV-infected cells fostered MoDCs to produce IL-6 (Fig. 5A) and activate NK cells and T cells regardless of their apoptotic alteration by TNF-alpha and cycloheximide (data not shown). There is also evidence showing that apoptotic lesions exist in the liver of patients with HCV hepatitis by histological examination.[26] Hence, it is acceptable that MoDCs take up apoptotic hepatocytes that contain HCV antigens and dsRNA in that lesion. Schulz et al.[8] reported that TLR3 in myeloid DCs promotes cross-priming to virus-infected cells using mouse bone marrow–derived DCs and Vero cells containing polyI:C or infected with dsRNA-producing picornavirus.[8] This model study, however, regrettably involves the process of xenogeneic cell-cell interaction. Nevertheless, our present study supports their notion in the human system and offers the possibility that myeloid DC maturation is reproduced by HCV-infected hepatocytes in HCV patients.

There have been many controversial reports about whether MoDCs were infected with HCV and deficient in the allostimulatory capacity in patients with chronic HCV infection.[10] A number of HCV proteins were suggested to affect MoDC function by overexpression studies. HCV core and E1 proteins inhibit the MoDC allostimulatory activity.[27] NS3/4A is a protease that inactivates the IFN-inducing pathways by cleaving the adapter molecules of RIG-I/MDA5 and TLR3, MAVS/Cardif/IPS-1/VISA,[11] and TICAM1/TRIF,[12] respectively. However, these proteins may not be authors for myeloid DC modulation, since HCV replication in MoDCs was not detected *in vitro* and HCV replicates in MoDCs from HCV patients were at very low copy numbers, if any.[10] Although defective MoDCs were reported to appear in HCV patients,[10] this may not merely be due to the DC-HCV interaction since HCV perturbs many cells and mediators in infected lesions.

In the HCV-infected apoptotic cells, there are HCV proteins as well as HCV-derived dsRNA. Therefore, the possibility still remains that not only dsRNA but also phagocytosed HCV proteins are involved in MoDC maturation. Although what happens in HCV natural infection is unclear, our study revealed that MoDC does not mature in response to lysates of HCV-infected apoptotic cells.

Sensor proteins for dsRNA reside in the cytoplasm as well as the cell surface.[7] In MoDCs, MDA5 and RIG-I may be engaged in sensors for HCV dsRNA in HCV-infected apoptotic cells. In this case, however, the dsRNA in phagosomes must pass through the membrane to encounter cytosolic RIG-I/MDA5. Thus, the possible interpretation is that apoptotic vesicles with HCV dsRNA are incorporated into the TLR3-bearing phagosome in MoDCs (Fig. 8C).

TLR3 is the receptor for dsRNA on the endosome membrane and engaged in MoDC maturation.[18] This maturation is inhibited by BAF and chloroquine, indicating that pH changes within intracellular compartments are critical for the process.[28] Opposing to these reports, treating MoDCs with BAF (Fig. 9) or chloroquine (data not shown) results in no inhibition of MoDC maturation in our HCV-incorporated vesicle studies. One possibility deduced from the BAF test is the presence of an alternative source for viral dsRNA recognition that is independent of endosomal acidification. Lipid rafts wherein HCV-infected apoptotic cells are phagocytosed (Fig. 9), may be associated with acidification-free MoDC maturation. Our data, including colocalization of dsRNA with TLR3 and partial blocking TLR3 with siRNA also suggested that TLR3 and HCV dsRNA assemble in the same compartment. Further studies on the dsRNA recognition facility in the phagosomes as well as possible participation of MDA5 and RIG-I in MoDC-NK reciprocal activation will be needed to clarify the mechanism of HCV-mediated MoDC maturation.

Acknowledgment: We are grateful to Drs. H. Oshiumi, M. Sasai, A. Ishii, K. Funami, and A. Matsuo in our laboratory for their experimental support. We appreciate Drs. K. Shimotohno (Kyoto University, Kyoto) and Y. Matsuura (Osaka University, Osaka) for their critical discussions. Thanks are also due to Drs. Chisari (The Scripps Research Institute, La Jolla, CA) for providing the cell line.

References

1. Poynard T, Yuen MF, Ratziu V, Lai CL. Viral hepatitis C. Lancet 2003; 362:2095-2100.
2. Haller O, Kochs G, Weber F. The interferon response circuit: induction and suppression by pathogenic viruses. Virology 2006;344:119-130.
3. Khakoo SI, Thio CL, Martin MP, Brooks CR, Gao X, Astemborski J, et al. HLA and NK cell inhibitory receptor genes in resolving hepatitis C virus infection. Science 2004;305:872-874.
4. Chang KM, Thimme R, Melpolder JJ, Oldach D, Pemberton J, Moorhead-Loudis J, et al. Differential CD4(+) and CD8(+) T-cell responsiveness in hepatitis C virus infection. HEPATOLOGY 2001;33:267-276.
5. Thimme R, Oldach D, Chang KM, Steiger C, Ray SC, Chisari FV. Determinants of viral clearance and persistence during acute hepatitis C virus infection. J Exp Med 2001;194:1395-1406.

6. Bigger CB, Brasky KM, Lanford RE. DNA microarray analysis of chimpanzee liver during acute resolving hepatitis C virus infection. J Virol 2001;75:7059-7066.
7. Akira S, Uematsu S, Takeuchi O. Pathogen recognition and innate immunity. Cell 2006;124:783-801.
8. Schulz O, Diebold SS, Chen M, Naslund TI, Nolte MA, Alexopoulou L, et al. Toll-like receptor 3 promotes cross-priming to virus-infected cells. Nature 2005;433:887-892.
9. Andrews DM, Andoniou CE, Scalzo AA, van Dommelen SL, Wallace ME, Smyth MJ, et al. Cross-talk between dendritic cells and natural killer cells in viral infection. Mol Immunol 2005;42:547-555.
10. Pachiadakis I, Pollara G, Chain BM, Naoumov NV. Is hepatitis C virus infection of dendritic cells a mechanism facilitating viral persistence? Lancet. Infect Dis 2005;5:296-304.
11. Li XD, Sun L, Seth RB, Pineda G, Chen ZJ. Hepatitis C virus protease NS3/4A cleaves mitochondrial antiviral signaling protein off the mitochondria to evade innate immunity. Proc Natl Acad Sci U S A 2005;102: 17717-17722.
12. Li K, Foy E, Ferreon JC, Nakamura M, Ferreon AC, Ikeda M, et al. Immune evasion by hepatitis C virus NS3/4A protease-mediated cleavage of the Toll-like receptor 3 adaptor protein TRIF. Proc Natl Acad Sci U S A 2005;102:2992-2997.
13. Wakita T, Pietschmann T, Kato T, Date T, Miyamoto M, Zhao Z. Production of infectious hepatitis C virus in tissue culture from a cloned viral genome. Nat Med 2005;11:791-796.
14. Zhong J, Gastaminza P, Cheng G, Kapadia S, Kato T, Burton DR, et al. Robust hepatitis C virus infection in vitro. Proc Natl Acad Sci U S A 2005;102:9294-9299.
15. Lee HK, Lund JM, Ramanathan B, Mizushima N, Iwasaki A. Autophagy-dependent viral recognition by plasmacytoid dendritic cells. Science 2007; 315:1398-1401.
16. Akazawa T, Ebihara T, Okuno M, Okuda Y, Shingai M, Tsujimura K, et al. Antitumor NK activation induced by the Toll-like receptor 3-TICAM-1 (TRIF) pathway in myeloid dendritic cells. Proc Natl Acad Sci U S A 2007;104:252-257.
17. Ebihara T, Masuda H, Akazawa T, Shingai M, Kikuta H, Ariga T, et al. NKG2D ligands are induced on human dendritic cells by TLR ligand stimulation and RNA virus infection. Int Immunol 2007;19:1145-1155.
18. Matsumoto M, Funami K, Tanabe M, Oshiumi H, Shingai M, Seto Y, et al. Subcellular localization of Toll-like receptor 3 in human dendritic cells J Immunol 2003;171:3154-3162.
19. Castet V, Fournier C, Soulier A, Brillet R, Coste J, Larrey D, et al. Alpha interferon inhibits hepatitis C virus replication in primary human hepatocytes infected in vitro. J Virol 2002;76:8189-8199.
20. Sosnovtsev SV, Prikhod'ko EA, Belliot G, Cohen JI, Green KY. Feline calicivirus replication induces apoptosis in cultured cells. Virus Res 200 94:1-10.
21. Prechtel AT, Turza NM, Theodoridis AA, Steinkasserer A. CD knockdown in monocyte-derived dendritic cells by small interfering RNA leads to a diminished T cell stimulation. J Immunol 2007;17 5454-5464.
22. Kaimori A, Kanto T, Kwang C, Limn, Komoda Y, Oki C, et al. Pseudotyp hepatitis C virus enters immature myeloid dendritic cells through th interaction with lectin. Virology 2004;324:74-83.
23. Heil F, Hemmi H, Hochrein H, Ampenberger F, Kirschning C, Akira S, et al. Species-specific recognition of single-stranded RNA via toll-like receptor 7 and 8. Science 2004;303:1526-1529.
24. Cormier EG, Durso RJ, Tsamis F, Boussemart L, Manix C, Olson WC, et al. L-SIGN (CD209L) and DC-SIGN (CD209) mediate transinfection of liver cells by hepatitis C virus. Proc Natl Acad Sci U S A 2004;101:1406 14072.
25. Yamada E, Montoya M, Schuettler CG, Hickling TP, Tarr AW, Vitelli A, et al. Analysis of the binding of hepatitis C virus genotype 1a and 1b E glycoproteins to peripheral blood mononuclear cell subsets. J Gen Vir 2005;86:2507-2512.
26. Kountouras J, Zavos C, Chatzopoulos D. Apoptosis in hepatitis C. J Vir Hepat 2003;10:335-342.
27. Sarobe P, Lasarte JJ, Zabaleta A, Arribillaga L, Arina A, Melero I, et a HCV structural proteins impair dendritic cell maturation and inhibit in vivo induction of cellular immune responses. J Virol 2003;77:1086 10871.
28. de Bouteiller O, Merck E, Hasan UA, Hubac S, Benguigui B, Trinchieri G, et al. Recognition of double-stranded RNA by human toll-like receptor and downstream receptor signaling requires multimerization and an acid pH. J Biol Chem 2005;280:38133-38145. 6.

JOURNAL OF VIROLOGY, Aug. 2008, p. 7964–7976 Vol. 82, No. 16
0022-538X/08/$08.00+0 doi:10.1128/JVI.00826-08

Interaction of Hepatitis C Virus Nonstructural Protein 5A with Core Protein Is Critical for the Production of Infectious Virus Particles[▽]

Takahiro Masaki,[1] Ryosuke Suzuki,[1] Kyoko Murakami,[1] Hideki Aizaki,[1] Koji Ishii,[1] Asako Murayama,[1] Tomoko Date,[1] Yoshiharu Matsuura,[2] Tatsuo Miyamura,[1] Takaji Wakita,[1] and Tetsuro Suzuki[1]*

Department of Virology II, National Institute of Infectious Diseases, Shinjuku-ku, Tokyo 162-8640, Japan,[1] and Department of Molecular Virology, Research Institute for Microbial Diseases, Osaka University, Suita-shi, Osaka 565-0871, Japan[2]

Received 17 April 2008/Accepted 22 May 2008

Nonstructural protein 5A (NS5A) of the hepatitis C virus (HCV) possesses multiple and diverse functions in RNA replication, interferon resistance, and viral pathogenesis. Recent studies suggest that NS5A is involved in the assembly and maturation of infectious viral particles; however, precisely how NS5A participates in virus production has not been fully elucidated. In the present study, we demonstrate that NS5A is a prerequisite for HCV particle production as a result of its interaction with the viral capsid protein (core protein). The efficiency of virus production correlated well with the levels of interaction between NS5A and the core protein. Alanine substitutions for the C-terminal serine cluster in domain III of NS5A (amino acids 2428, 2430, and 2433) impaired NS5A basal phosphorylation, leading to a marked decrease in NS5A-core interaction, disturbance of the subcellular localization of NS5A, and disruption of virion production. Replacing the same serine cluster with glutamic acid, which mimics the presence of phosphoserines, partially preserved the NS5A-core interaction and virion production, suggesting that phosphorylation of these serine residues is important for virion production. In addition, we found that the alanine substitutions in the serine cluster suppressed the association of the core protein with viral genome RNA, possibly resulting in the inhibition of nucleocapsid assembly. These results suggest that NS5A plays a key role in regulating the early phase of HCV particle formation by interacting with core protein and that its C-terminal serine cluster is a determinant of the NS5A-core interaction.

Hepatitis C virus (HCV) infection is a major public health problem and is prevalent in about 200 million people worldwide (27, 40, 42). Current protocols for treating HCV infection fail to produce a sustained virological response in as many as half of treated individuals, and many cases progress to chronic liver disease, including chronic hepatitis, cirrhosis, and hepatocellular carcinoma (15, 31, 35, 43).

HCV is a positive-strand RNA virus classified in the *Hepacivirus* genus within the *Flaviviridae* family (55). Its approximately 9.6-kb genome is translated into a single polypeptide of about 3,000 amino acids (aa), in which the structural proteins core, E1, and E2 reside in the N-terminal region. A crucial function of core protein is assembly of the viral nucleocapsid. The amino acid sequence of this protein is well conserved among different HCV strains compared to other HCV proteins. The nonstructural (NS) proteins NS3-NS5B are considered to assemble into a membrane-associated HCV RNA replicase complex. NS3 possesses the enzymatic activities of serine protease and RNA helicase, and NS4A serves as a cofactor for NS3 protease. NS4B plays a role in the remodeling of host cell membranes, probably to generate the site for the replicase assembly. NS5B functions as the RNA-dependent RNA polymerase. NS5A is known to play an important but undefined role in viral RNA replication.

NS5A is a phosphoprotein that can be found in basally phosphorylated (56 kDa) and hyperphosphorylated (58 kDa) forms (49). Comparative sequence analyses and limited proteolysis of recombinant NS5A have demonstrated that NS5A is composed of three domains (52). Domain I is relatively conserved among HCV genotypes compared to domains II and III. Analysis of the crystal structure of the conserved domain I that immediately follows the membrane-anchoring α-helix localized at the N terminus revealed a dimeric structure (53). The interface between protein molecules is characterized by a large, basic groove, which has been proposed as a site of RNA binding. In fact, its RNA binding property has been demonstrated biochemically (17). Domains II and III of NS5A are far less understood. Domain II contains a region referred to as the interferon sensitivity determining region, and this region and its C-terminal 26 residues have been shown to be essential for interaction with the interferon-induced, double-stranded RNA-dependent protein kinase (6–10, 38, 39, 48). Domain III includes a number of potential phosphoacceptor sites and is most likely involved in basal phosphorylation. This domain tolerates insertion of large heterologous sequences such as green fluorescent protein (GFP) and is not required for function of NS5A in HCV RNA replication (1, 34). However, a study with the recently established productive HCV cell culture system using genotype 2a isolate JFH-1 (28, 56, 58) demonstrated that while insertion of GFP within the NS5A region does not affect RNA replication, it does produce marked decreases in the production of infectious virus particles (41). This suggests that the C-terminal region of NS5A may affect virus particle production independent of RNA replication. Re-

* Corresponding author. Mailing address: Department of Virology II, National Institute of Infectious Diseases, 1-23-1 Toyama, Shinjuku-ku, Tokyo 162-8640, Japan. Phone: 81 3 5285 1111. Fax: 81 3 5285 1161. E-mail: tesuzuki@nih.go.jp.

▽ Published ahead of print on 4 June 2008.

cently, Miyanari et al. reported that the association of core protein with the NS proteins and replication complexes around lipid droplets (LDs) is critical for producing infectious viruses (33).

In the present study, we demonstrated that NS5A is a prerequisite for HCV particle production via its interaction with core protein, and we identified serine residues in the C-terminal region of NS5A that play an important role in virion production. Substitution of the serine residues with alanine residues inhibited not only the interaction of NS5A with core protein but also HCV RNA-core association and led to a decrease in HCV particle production with no effect on RNA replication.

MATERIALS AND METHODS

DNA construction. Plasmids pJFH1, which contains the full-length JFH-1 cDNA downstream of the T7 RNA promoter sequence, and pSGR-JFH1/Luc, in which the neomycin resistance gene of pSGR-JFH1 has been replaced by the firefly luciferase reporter gene, have been previously described (24, 56). To generate the fluorochrome gene-tagged full-length JFH-1 plasmid, pJFH1/NS5A-GFP, the region encompassing the RsrII site of NS5A and the BsrGI site of NS5B was amplified by PCR, the amplification product was cloned into pGEM-T Easy vector (Promega, Madison, WI), and the resultant plasmid was designated pGEM-JFH1/RsrII-BsrGI. A GFP reporter gene was amplified by PCR from pGreen Lantern-1 (Invitrogen, Carlsbad, CA) with primers containing the XhoI sequence and inserted, after restriction digestion with XhoI, into the XhoI site of pGEM-JFH1/RsrII-BsrGI. The resulting plasmid was digested by RsrII and BsrGI and ligated into pJFH1 similarly digested by RsrII and BsrGI to produce pJFH1/NS5A-GFP. For generation of the fluorochrome gene-tagged subgenomic reporter plasmid, pJFH1/NS5A-GFP was digested by RsrII and SnaBI and ligated into pSGR-JFH1/Luc similarly digested by RsrII and SnaBI. The mutations in the NS5A gene were generated by oligonucleotide-directed mutagenesis (57). To construct plasmids expressing N-terminally FLAG-tagged HCV core protein or hemagglutinin (HA)-tagged NS5A, DNA fragments encoding core protein or NS5A (wild type or mutants) were generated from the full-length JFH-1 cDNA by PCR. The core protein coding sequence, together with a FLAG sequence linked to its N terminus, was cloned into the pCAGGS vector (37). The coding sequences of NS5A, together with an HA sequence linked to their N termini, were also cloned into pCAGGS vectors. All PCR products were confirmed by automated nucleotide sequencing with an ABI Prism 3130 Avant Genetic Analyzer (Applied Biosystems, Tokyo, Japan).

Cells and viruses. The human hepatoma cell line, Huh-7, and JFH1/4-1 cells, which are Huh-7 cells carrying a subgenomic replicon of JFH-1 (32), were maintained in Dulbecco's modified Eagle's medium (DMEM) supplemented with minimal essential medium nonessential amino acids (Invitrogen), 100 units/ml of penicillin, 100 μg/ml of streptomycin, and 10% fetal bovine serum (FBS) at 37°C in a 5% CO_2 incubator. Huh/c-p7 cells, which are Huh-7 cells stably expressing the proteins core to p7 derived from the JFH-1 strain (18), were incubated in DMEM containing 300 μg/ml of zeocin (Invitrogen). HCV particles derived from JFH-1 were produced by transient transfection of Huh-7 cells with in vitro transcribed RNA, as described previously (56, 58). Recombinant vaccinia virus strain DIs, which expresses the bacteriophage T7 RNA polymerase under the control of the vaccinia virus early/late promoter P7.5, was generated and propagated as previously described (19).

DNA transfection, immunoprecipitation (IP), and immunoblotting. For coexpression of FLAG-tagged core protein and HA-tagged NS5A, cells were seeded onto 35-mm wells of a six-well cell culture plate and cultured overnight. Plasmid DNAs (2 μg) were transfected into cells using TransIT-LT1 transfection reagent (Mirus, Madison, WI). Cells were harvested at 48 h posttransfection, washed three times with 1 ml of ice-cold phosphate-buffered saline (PBS), and suspended in 0.25 ml lysis buffer (20 mM Tris-HCl [pH 7.4] containing 135 mM NaCl, 1% Triton X-100, 0.05% sodium dodecyl sulfate [SDS], and 10% glycerol) supplemented with 50 mM NaF, 5 mM Na_3VO_4, 1 μg/ml leupeptin, and 1 mM phenylmethylsulfonyl fluoride (PMSF). Cell lysates were sonicated at 4°C for 5 min, incubated for 30 min at 4°C, and centrifuged at 14,000 × *g* for 5 min at 4°C. After preclearing, the supernatant was immunoprecipitated with 10 μl of anti-FLAG M2-agarose beads (Sigma, St. Louis, MO). For expression of the full-length HCV polyprotein, Huh-7 cells transfected with 10 μg of in vitro transcribed RNAs by electroporation were resuspended in 20 or 30 ml of culture medium, and 10-ml aliquots were seeded into 100-mm culture dishes. At 72 h posttransfection, the cells were incubated in 0.5 ml of lysis buffer (20 mM Tris-HCl [pH 7.4] containing 135 mM NaCl, 1% Triton X-100, 0.5% sodium deoxycholate, and 10% glycerol) supplemented with 50 mM NaF, 5 mM Na_3VO_4, 1 μg/ml leupeptin, and 1 mM PMSF. After preclearing, the supernatant was immunoprecipitated with 5 μg of polyclonal anti-NS5A antibody (34a) or polyclonal anti-C/EBPβ antibody (Santa Cruz Biotechnology, Santa Cruz, CA), and 20 μl of protein G-agarose beads (Invitrogen). The immunocomplex was precipitated with the beads by centrifugation at 800 × *g* for 30 s and then was washed five times with lysis buffer by centrifugation. The proteins binding to the beads were boiled in 20 μl of SDS sample buffer and then subjected to SDS–12.5% polyacrylamide gel electrophoresis (PAGE). The proteins were transferred onto a polyvinylidene difluoride membrane (Immobilon; Millipore, Bedford, MA) and then reacted with a primary antibody and a secondary horseradish peroxidase-conjugated antibody. The immunocomplexes were visualized with an ECL Plus Western Blotting Detection System (GE Healthcare, Buckinghamshire, United Kingdom) and detected using an LAS-3000 imaging analyzer (Fujifilm, Tokyo, Japan).

In vitro synthesis of HCV RNA and RNA transfection. Plasmid DNAs were digested with XbaI and treated with mung bean nuclease (New England Biolabs, Ipswich, MA) to remove the four terminal nucleotides, resulting in the correct 3′ end of the HCV cDNA. Digested DNAs were purified and used as templates for RNA synthesis. HCV RNA was synthesized in vitro using a MEGAscript T7 kit (Ambion, Austin, TX). Synthesized RNA was treated with DNase I (Ambion), followed by acid guanidinium thiocyanate-phenol-chloroform extraction to remove any remaining template DNA. Synthesized HCV RNAs were used for electroporation. Trypsinized Huh-7 cells were washed with Opti-MEM I reduced-serum medium (Invitrogen) and resuspended at 3×10^6 cells/ml with Cytomix buffer (54). RNA was mixed with 400 μl of cell suspension and transferred into an electroporation cuvette (Precision Universal Cuvettes; Thermo Hybaid, Middlesex, United Kingdom). Cells were then pulsed at 260 V and 950 μF using a Gene Pulser II unit (Bio-Rad, Hercules, CA). Transfected cells were immediately transferred onto six-well culture plates or 100-mm culture dishes.

Luciferase assay. Cells were harvested at different time points posttransfection of subgenomic reporter replicons and lysed in passive lysis buffer (Promega). The luciferase activity in cells was determined using a luciferase assay system (Promega).

Quantification of HCV core protein. HCV core protein in transfected cells or cell culture supernatants was quantified using a highly sensitive enzyme immunoassay (Ortho HCV antigen ELISA Kit; Ortho Clinical Diagnostics, Tokyo, Japan). To determine intracellular core protein amounts, cell lysates were prepared as described previously (41). To determine the efficiency of core protein release, the ratio of extracellular core protein to total core protein (the sum of intra- and extracellular core protein amounts) was calculated.

Intra- and extracellular infectivity assay. Culture supernatants were harvested 72 h posttransfection, and virus titers were determined by a 50% tissue culture infectious dose ($TCID_{50}$) assay as described previously (28, 46). Virus titration was performed by seeding naïve Huh-7 cells in 96-well plates at a density of 1×10^4 cells/well. Samples were serially diluted fivefold in complete growth medium and used to infect the seeded cells (six wells per dilution). At 72 h after infection, the inoculated cells were fixed and immunostained with a mouse monoclonal anti-core protein antibody (2H9) (56), followed by an Alexa Fluor 488-conjugated anti-mouse immunoglobulin G (IgG) (Invitrogen). Wells that showed at least one core protein-expressing cell was counted as positive. Cell-associated infectivity was determined essentially as described previously (12, 47). Briefly, cells were extensively washed with PBS, scraped, and centrifuged for 3 min at 120 × *g*. Cell pellets were resuspended in 1 ml of DMEM containing 10% FBS and subjected to four cycles of freezing and thawing using dry ice and a 37°C water bath. Samples were then centrifuged at 2,400 × *g* for 10 min at 4°C to remove cell debris, and cell-associated infectivity was determined by $TCID_{50}$ assay.

Expression of HCV proteins using vaccinia viruses, metabolic labeling of cells, and radioimmunoprecipitation analysis. Metabolic labeling of cells and radioimmunoprecipitation analysis were performed as described by Huang et al. (17) with some modifications. A total of 4×10^5 Huh-7 cells were seeded onto each well of six-well cell culture plates and cultured overnight. A 2-μg amount of subgenomic replicon DNAs carrying defined NS5A mutations was transfected into cells using TransIT-LT1 transfection reagent, and at 12 h posttransfection the cells were then infected at a multiplicity of infection of 10 with recombinant vaccinia viruses expressing the T7 RNA polymerase. After 40 h of transfection, cells were incubated in methionine- and cysteine-deficient DMEM (Invitrogen) or phosphate-deficient DMEM (Invitrogen) for 2 h and labeled for 6 h with [^{35}S]methionine and [^{35}S]cysteine (200 μCi/well; GE Healthcare) or

[^{32}P]orthophosphate (250 μCi/well; GE Healthcare). The cells were then washed twice with cold PBS and lysed with SDS lysis buffer (50 mM Tris-HCl [pH 7.6], 0.5% SDS, 1 mM EDTA, 20 μg/ml of PMSF). The cell lysates were passed through a 27-gauge needle several times to shear cellular DNA. After a 10-min incubation at 75°C, the lysates were clarified by centrifugation and diluted five-fold with HNAET buffer (50 mM HEPES [pH 7.5], 150 mM NaCl, 0.67% bovine serum albumin, 1 mM EDTA, 0.33% Triton X-100). After preclearing by incubation with 20 μl of protein G-agarose beads for 1 h at 4°C, the supernatant was incubated with 2 μg of rabbit polyclonal anti-NS5A antibody overnight at 4°C. A 20-μl aliquot of protein G agarose beads was further added and incubated for 2 h at 4°C. The cell pellets were washed three times with 0.5 ml of HNAETS buffer (HNAET containing 0.5% SDS), followed by washing once with 0.5 ml of HNE buffer (50 mM HEPES [pH 7.5], 150 mM NaCl and 1 mM EDTA). After treatment with or without λ protein phosphatase (New England Biolabs), the cell pellets were suspended in 20 μl of SDS sample buffer and boiled for 10 min. The proteins were resolved on 10% SDS-polyacrylamide gels and analyzed by autoradiography.

Subcellular fractionation analysis. All steps were carried out at 4°C in the presence of a protease inhibitor cocktail (Complete; Roche, Mannheim, Germany) as described previously (20), with some modifications. Cells were suspended in four cell volumes of homogenization buffer (50 mM NaCl, 10 mM triethylamine [pH 7.4], 1 mM EDTA), snap frozen in liquid nitrogen, stored at −80°C, and thawed in a water bath at room temperature. Supernatants (0.4 ml) were layered on linear 10-ml iodixanol gradients from 2.5 to 25% and centrifuged at 37,000 rpm for 3.5 h in an SW41 rotor (Beckman, Fullerton, CA), followed by collection of 0.8-ml fractions from the top. Each fraction was concentrated by Centricon YM30 (Millipore), separated by SDS-PAGE, and immunoblotted with a rabbit polyclonal anti-calnexin antibody (Stressgen Biotechnologies, Victoria, Canada), a mouse monoclonal anti-adipose differentiation-related protein (ADRP) antibody (Progen Biotechnik, Heidelberg, Germany), or a rabbit polyclonal anti-NS5A antibody. The core protein amount in each fraction was also determined by enzyme-linked immunosorbent assay (ELISA).

IP-RT-PCR. The process of cell lysis to RNA purification was carried out essentially as described by Johnson et al. (21) with some modifications. A total of 3×10^6 Huh-7 cells were transfected with 10 μg of in vitro transcribed HCV RNAs and resuspended in 20 or 30 ml of culture medium, after which 10-ml aliquots were seeded into 100-mm culture dishes. At 72 h posttransfection, the cells were scraped and incubated in 500 μl of hypotonic buffer (10 mM HEPES [pH 7.6], 1.5 mM $MgCl_2$, 10 mM KCl, 0.2 mM PMSF) per dish. The cells were passed through a 20-gauge needle several times, lysed with Nonidet P-40 at a final concentration of 1%, and incubated on ice for an additional 10 min. After centrifugation at 4,000 × *g* at 4°C for 15 min, glycerol was added to the supernatants at a final concentration of 5%. The cell lysates were incubated with 20 μl of protein G-agarose beads for 30 min at room temperature. After the cell lysates were removed from protein G-agarose beads, 5 μg of mouse monoclonal anti-core protein antibody or normal mouse IgG (Sigma) as a negative control was added, and samples were incubated for an additional 1 h at room temperature. A 20-μl aliquot of protein G-agarose beads per sample was added to the cell lysates and incubated for 1 h. After incubation, the beads were washed three times with wash buffer (10 mM Tris-HCl [pH 7.6], 100 mM KCl, 5 mM $MgCl_2$, and 1 mM dithiothreitol) and eluted in 100 μl of elution buffer (50 mM Tris-HCl [pH 8.0], 1% SDS, and 10 mM EDTA) at 65°C for 10 min. After treatment with 100 μg of proteinase K at 37°C for 30 min, the RNAs in immunocomplexes were isolated by acid guanidinium thiocyanate-phenol-chloroform extraction. Reverse transcriptase PCR (RT-PCR) was carried out using random hexamer and Superscript II RT (Invitrogen), followed by nested PCR with LA *Taq* DNA polymerase (TaKaRa, Shiga, Japan) and primer sets amplifying the fragments of nucleotides (nt) 129 to 2367 and nt 7267 to 9463 of the JFH-1 genome. To amplify the fragment of nt 129 to 2367, the sense primer 5′-CTGTGAGGAAC TACTGTCTT-3′ and the antisense primer 5′-TCCACGATGTTCTGGTGAA G-3′ were used for first-round PCR; the sense primer 5′-CGGGAGAGCCAT AGTGG-3′ and the antisense primer 5′-CATTCCGTGGTAGAGTGCA-3′ were used for second-round PCR. To amplify the fragment of nt 7267 to 9463, the sense primer 5′-GTCCAGGGTGCCCGTTCTGGACT-3′ and the antisense primer 5′-GCGGCTCACGGACCTTTCAC-3′ were used for first-round PCR; the sense primer 5′-CACCGTTGCTGGTTGTGCT-3′ and the antisense primer 5′-GTGTACCTAGTGTGTGCCGCTCTA-3′ were used for second-round PCR.

Indirect immunofluorescence analysis. Cells incubated for 3 days after transfection with JFH-1 RNAs were seeded in an eight-well chamber slide (BD Biosciences, San Jose, CA) and cultured overnight. The adherent cells were washed twice with PBS and fixed with 4% paraformaldehyde at room temperature. After a washing step with PBS, the cells were permeabilized with PBS containing 0.3% Triton X-100 and 2% FBS for 1 h at room temperature and stained with a rabbit polyclonal anti-NS5A antibody and a mouse monoclonal anti-core protein antibody. The fluorescent secondary antibodies were Alexa Fluor 488- or Alexa Fluor 555-conjugated anti-rabbit or anti-mouse IgG antibodies (Invitrogen). Analyses of JFH-1 were performed on a Zeiss confocal laser scanning microscope LSM 510 (Carl Zeiss, Oberkochen, Germany).

RESULTS

Mutations of serine residues at the NS5A C terminus impair basal phosphorylation but have little effect on viral RNA replication. As demonstrated in a previous study, insertion of GFP into the NS5A C terminus does not significantly affect viral RNA replication but reduces the generation of infectious HCV particles (41). The C-terminal region of NS5A contains highly conserved serine residues that are involved in basal phosphorylation (1, 23, 49). To examine the involvement of the serine clusters (cluster 3-A [CL3A] and cluster 3-B [CL3B]) in the C-terminal region of NS5A in HCV particle production, we created mutated HCV genomes as well as subgenomic replicons carrying alanine substitutions for the conserved serine residues at aa 2384, 2388, 2390, and 2391 (residues are numbered according to the positions within the original JFH-1 polyprotein) (CL3A/SA); at aa 2428, 2430, and 2433 (CL3B/SA); or an in-frame deletion spanning aa 2384 to 2433 (Δ2384–2433) (Fig. 1). A construct with an in-frame insertion of GFP (NS5A-GFP) was also generated as described previously for the Con1 isolate (34).

First, we analyzed the effects of the NS5A mutations on HCV RNA replication using a transient RNA replication assay using subgenomic luciferase reporter replicons (Fig. 2A) and found that the serine-to-alanine substitutions (CL3A/SA and CL3B/SA) did not affect viral RNA replication. NS5A-GFP and Δ2384–2433 slightly reduced RNA replication, indicating that the mutations of the NS5A C terminus tested in this study do not critically affect RNA replication, which is consistent with previous reports (1, 34, 51).

Next, the phosphorylation status of the mutated NS5A was analyzed as described in Materials and Methods (Fig. 2B). NS5A was isolated from radiolabeled cells by IP and analyzed either directly by SDS-PAGE or after treatment with λ protein phosphatase. Analysis of ^{32}P-radiolabeled proteins revealed that the CL3A/SA, CL3B/SA, and Δ2384–2433 mutations resulted in marked reduction of basal phosphorylation (Fig. 2B, compare lane 1 with lanes 3, 5, and 7 in the top panel). All ^{32}P-labeled NS5A proteins were sensitive to treatment with phosphatase (lanes 2, 4, 6, and 8). The possibility that loss of signal after dephosphorylation was due to contaminating proteases present in the phosphatase preparations can be ruled out because no degradation of the ^{35}S-labeled proteins was observed (Fig. 2B, bottom panel). These results suggest that mutations in the C-terminal serine cluster of NS5A impair basal phosphorylation but have no significant effect on viral RNA replication.

Effect of mutations introduced into the NS5A C terminus on the production of infectious HCV particles. To analyze HCV particle production from cells transfected with the in vitro transcribed viral genomic RNAs, we harvested supernatants and cells at 4, 24, 48, 72, and 96 h posttransfection and measured the amounts of core protein. As shown in Fig. 3A, comparable amounts of core proteins were detected in all transfected cells 4 h after transfection, reflecting unchanged

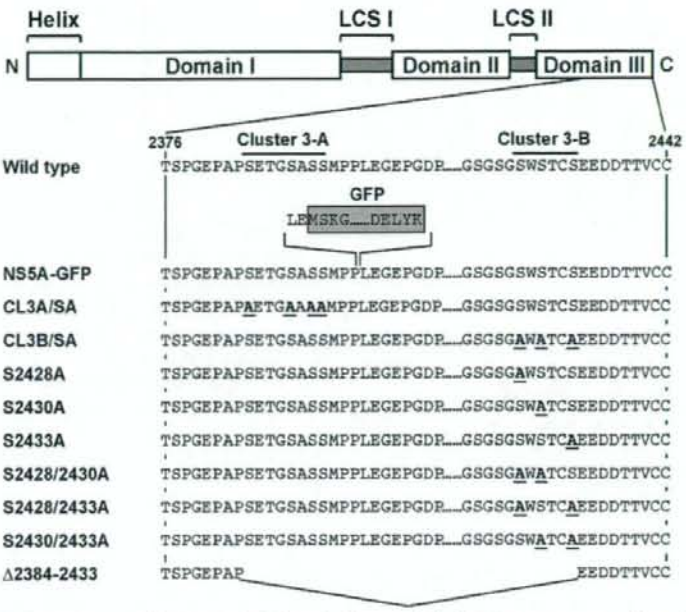

FIG. 1. Structures of HCV constructs used in this study. Schematic diagram of the NS5A structure according to Tellinghuisen et al. (52) is shown in the top panel. The three domains are indicated by white boxes and are separated by trypsin-sensitive regions with presumably low structural complexity (low-complexity sequence [LCS]). The numbers indicate amino acid residues within the original JFH-1 polyprotein. The names listed on the left represent full-length HCV constructs, subgenomic reporter replicons, or N-terminally HA-tagged NS5A constructs used in this study. NS5A-GFP carries a GFP insertion between aa 2394 and 2395 as indicated by a shaded box. CL3A/SA and CL3B/SA carry several serine-to-alanine substitutions in the NS5A C terminus constructed as described previously (1). HCV constructs from S2428A to S2430/2433A carry single or double serine-to-alanine substitutions generated by modification of the CL3B/SA construct. The Δ2384–2433 mutant possesses an in-frame deletion in the C-terminal region of NS5A. Amino acid substitutions are marked in bold and underlined. N and C represent N terminus and C terminus, respectively.

transfection efficiencies, and the kinetics of intracellular core protein levels was similar among transfectants. By contrast, core protein released from cells transfected either with the mutated genome of CL3B/SA, Δ2384–2433, or NS5A-GFP was more than 10-fold lower than that for the wild-type JFH-1 or CL3A/SA (Fig. 3B). Figure 3C shows the efficiency of core protein release from each transfectant, which is expressed as a percentage of the extracellular core protein level relative to the amount of total core protein (the sum of intra- and extracellular core protein). Core protein release efficiency with the wild type and CL3A/SA was 2 to 13% at 48 to 96 h after transfection, while only 1% or less of core protein was released in the cases of CL3B/SA, Δ2384–2433, and NS5A-GFP strains.

To further investigate production and release of infectious virus particles, naïve Huh-7 cells were infected with culture supernatants of cells harvested 72 h posttransfection, and infectious virus titers were determined by $TCID_{50}$ assay at 72 h after infection. Figure 3D shows that release of infectious virus particles from cells transfected with the genome of CL3B/SA or Δ2384–2433 mutants was markedly reduced (about 10,000-fold) compared to that from wild-type- or CL3A/SA-transfected cells (white bars). To examine whether such a decrease in infectious HCV in the culture supernatants was attributable to defective virion assembly or impaired release of virions, we determined cell-associated infectivity (Fig. 3D). Production of intracellular infectious virions in CL3B/SA- and Δ2384-2433-transfected cells was strongly impaired in comparison with that in wild-type-transfected (~1,000-fold) and CL3A/SA-transfected (~100-fold) cells. Thus, the results suggest a potential role for the serine cluster at aa 2428, 2430, and 2433 of NS5A in assembly of infectious HCV particles. Among the NS5A mutations tested, CL3B/SA is of particular interest because this mutation leads to a marked reduction in HCV production with no impact on viral RNA replication.

Serine residues at aa 2428, 2430, and 2433 are important for the interaction between NS5A and core protein. Miyanari et al. reported that the association of core protein with NS proteins is critical for infectious HCV production and that mutations of the core protein and NS5A that cause these proteins to fail to associate with each other impair the production of infectious virus (33). Based on these observations and the findings noted above, we hypothesize that NS5A plays a key role in recruiting viral RNA, which is synthesized at the viral replication complex, to nucleocapsid formation via interaction between the NS5A C-terminal region and the core protein. To prove this, we analyzed the interaction of NS5A with the core protein by coimmunoprecipitation experiments. HA-tagged NS5A constructs carrying defined mutations were generated (Fig. 1) and coexpressed with the FLAG-tagged core protein in Huh-7 cells. As shown in Fig. 4A, coimmunoprecipitation of NS5A

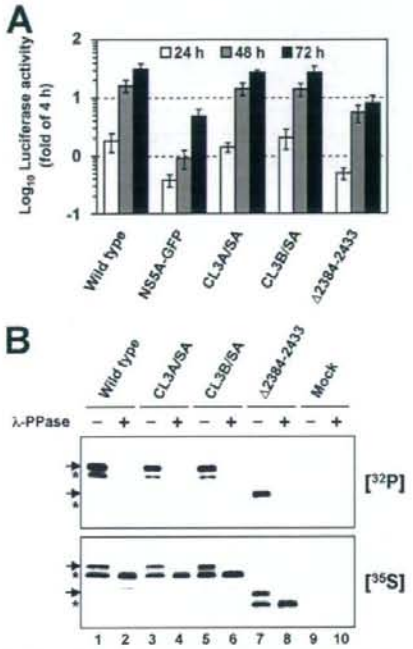

FIG. 2. Mutations at the C terminus of NS5A impair basal phosphorylation and have only a minor impact on RNA replication. (A) Replication of given mutants in transfected Huh-7 cells as determined by luciferase reporter assays performed at 24, 48, and 72 h posttransfection (white, gray, and black bars, respectively). Values given were normalized for transfection efficiency using the luciferase activity determined 4 h after transfection, which was set to 1. Mean values of quadruplicate measurements and the standard deviations are given. (B) Phosphorylation analysis of NS5A using the vaccinia virus T7 hybrid system. NS3-to-NS5B polyprotein fragments carrying the mutations specified above the lanes were transfected into Huh-7 cells, and proteins were radiolabeled with [^{32}P]orthophosphate or [^{35}S]methionine and [^{35}S]cysteine. NS5A proteins were isolated by IP and separated by SDS-PAGE (10% polyacrylamide). Mock-transfected cells served as a negative control (lanes 9 and 10). Half of the samples were treated with λ protein phosphatase (λ-PPase) (+) whereas the other half was mock treated (−) prior to SDS-PAGE. Arrows and asterisks indicate hyperphosphorylated and basally phosphorylated forms, respectively.

with the core protein was observed in cells expressing the wild-type NS5A and the CL3A/SA-mutated NS5A, but the amount of immunoprecipitated NS5A in the CL3A/SA-expressing cells was slightly lower than that in the wild-type-expressing cells. In contrast, the CL3B/SA- or the Δ2384-2433-mutated NS5A coimmunoprecipitated with the core protein only slightly or not at all.

We further examined the interaction of NS5A with core protein in cells expressing HCV genomes. At 72 h posttransfection with the wild type or CL3B/SA, cells were harvested and immunoprecipitated with an anti-NS5A antibody or an anti-C/EBPβ antibody as a negative control, followed by immunoblotting. Under these experimental conditions, the amount of extracellular core protein released from cells transfected with the CL3B/SA genome was about 10-fold lower than that for the wild type, although comparable amounts of intracellular core protein were observed in both transfectants (Fig. 4B, left panels). As shown in the right panels of Fig. 4B, the core protein was specifically coimmunoprecipitated with NS5A in cells expressing the wild-type JFH-1 genome but not with the mutated NS5A in cells expressing the CL3B/SA genome. These results demonstrate that NS5A interacts with the core protein in cells producing infectious particles and that serine residues at aa 2428, 2430, and 2433 are important to the success of this interaction.

Two serine residues among aa 2428, 2430, and 2433 are responsible for regulating the interaction of NS5A with the core protein as well as HCV particle production. To further determine the critical residues in the C-terminal serine cluster of NS5A responsible for HCV particle production, we replaced one or two serine residues in the region with alanine (Fig. 1) and investigated which serine-to-alanine substitution influenced HCV particle production. Core protein levels in cells transfected with any construct were comparable over 4 days after transfection, indicating similar efficiencies of transfection and RNA replication from each construct (data not shown). As shown in Fig. 5A, we observed a slight delay in the kinetics of core protein release from cells transfected with the single-substitution genomes, S2428A, S2430A, and S2433A, up to 48 or 72 h posttransfection. However, core protein release from these cells reached comparable levels to that for the wild type at 96 h after transfection. In the cases of the double-substitution mutants (Fig. 5B), core protein release from cells transfected with the double-substitution genomes was markedly reduced, with 10- to 30-fold decreases compared to that for wild type observed. The kinetics of core protein release were similar to that for CL3B/SA.

Interaction of NS5A carrying single or double serine-to-alanine substitutions with the core protein was investigated by coimmunoprecipitation analysis using HA-tagged NS5A constructs. NS5A mutants carrying a single substitution were coimmunoprecipitated with the core protein (Fig. 5C), while none of the double-substitution NS5A mutants or the triple-substitution mutant, CL3B/SA, coimmunoprecipitated with the core protein (Fig. 5D). These results suggest that at least two serine residues in the C-terminal serine cluster of NS5A (aa 2428, 2430, and 2433) are necessary for the interaction between NS5A and the core protein as well as for regulation of HCV particle production and that there is positive correlation between their interaction and the amount of core protein released.

Glutamic acid partially substitutes for serine phosphorylation in the interaction of NS5A with the core protein and virus production. A consequence of phosphorylation is the addition of negative charge to a protein. In some cases, phosphoserine can be mimicked by glutamic or aspartic acid (14). To determine whether the introduction of negative charges into aa 2428, 2430, and 2433 instead of phosphoserines positively regulates the interaction of NS5A with the core protein and virus production, we replaced the serine residues with glutamic acid residues and constructed the CL3B/SE and S2428/2430E mutants (Fig. 6A). Cells transfected with the double-glutamic acid substitution, S2428/2430E, exhibited similar kinetics to the wild-type-transfected cells and released ~22-fold more core protein than S2428/2430A-transfected cells by 96 h posttransfection (Fig. 6B). In contrast,

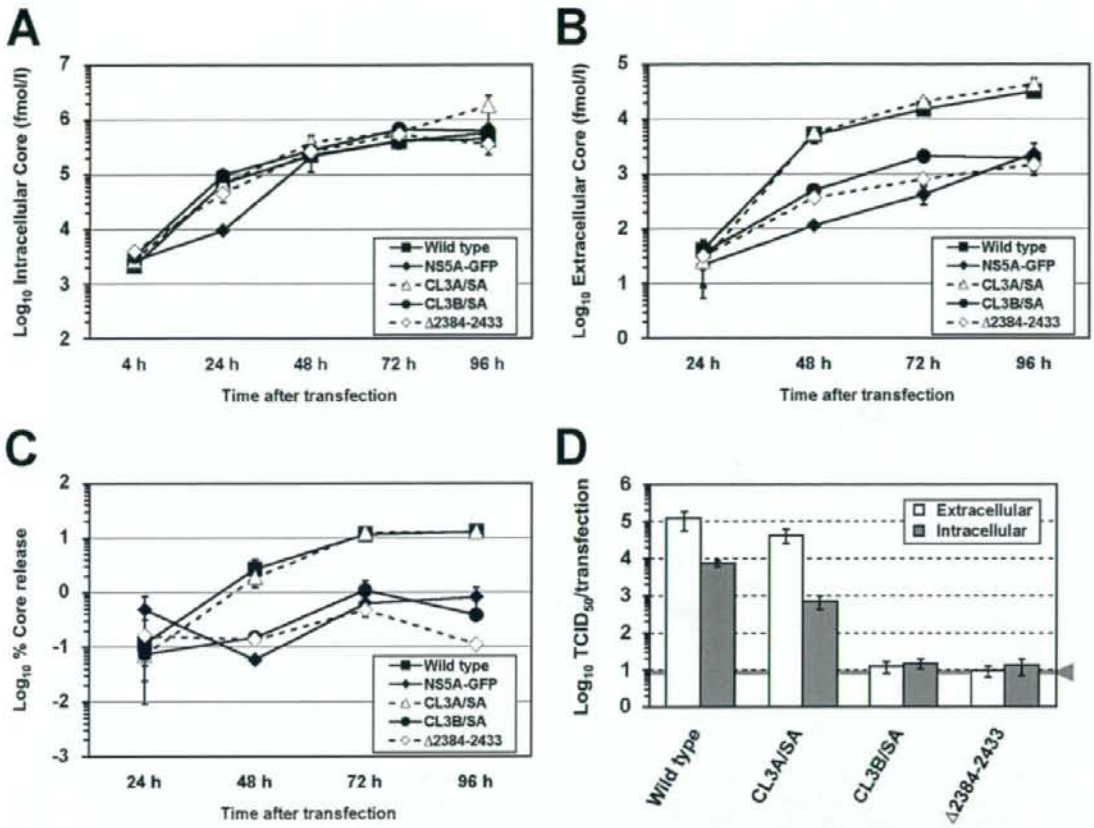

FIG. 3. Effect of mutations introduced into the NS5A C terminus on the production of infectious HCV particles. (A) Intracellular levels of core protein measured at various time points after transfection. A total of 3×10^6 Huh-7 cells were transfected with 10 μg of in vitro-transcribed HCV RNAs specified in the inset and resuspended in 10 ml of culture medium, after which 2-ml aliquots were seeded into each well of a six-well culture plate. The cells were harvested at different time points between 4 h and 96 h posttransfection, and then 500 μl of cell lysate per well was prepared. After centrifugation, supernatants were processed for a core protein-specific ELISA. (B) Release of core protein from cells transfected with the HCV genomes specified in the inset. Cell culture supernatants harvested from cells given in panel A were analyzed by a core protein ELISA. (C) Efficiency of core protein release from cells transfected with the HCV genomes specified in the inset. The percent core protein release (vertical axis) indicates the percentage of released core protein in relation to total core protein (the sum of intra- and extracellular core protein) calculated for each time point. (D) Infectivity of virus particles contained in supernatants and cells after transfection with mutants specified below the graph. Culture supernatants and cells were harvested 72 h posttransfection, and extracellular (white bars) and intracellular infectivity (gray bars) levels were determined by $TCID_{50}$ assay. The gray line and arrowhead represent the detection limit of the limiting dilution assay. Mean values and standard deviations for at least triplicates are shown in all panels.

the transfectant with the triple glutamic acid substitution, CL3B/SE, showed similar trends to that of CL3B/SA. In the coimmunoprecipitation experiments with FLAG-tagged core protein and HA-tagged NS5A constructs (Fig. 6C), S2428/2430E, but not S2428/2430A, restored the ability of NS5A to interact with the core protein up to a similar level to that of wild type. As expected, neither CL3B/SE nor CL3B/SA coimmunoprecipitated with the core protein. Taken together, these results indicate that negative charges at aa 2428 and 2430 preserve the ability of NS5A to interact with the core protein and positively regulate virus production. However, the data of the CL3B/SE mutant indicate that it is likely that negative charges alone are not sufficient to enhance either the interaction of NS5A with the core protein or virus production.

Subcellular localization of NS5A and core protein in Huh-7 cells expressing HCV genomes. The coimmunoprecipitation experiments described above indicate that the wild-type NS5A but not the CL3B/SA mutant interacts with the core protein. To evaluate the NS5A-core protein interaction in intact cells, we examined the subcellular localization of NS5A with the core protein by immunofluorescence analysis. NS5A colocalized with the core protein in cells transfected with the JFH-1 wild type (Fig. 7A), whereas their colocalization was rarely observed in cells transfected with the CL3B/SA RNA (Fig. 7B).

To further analyze the subcellular compartments for the localization of NS5A and core protein in cytoplasmic membrane structures, including the endoplasmic reticulum (ER) and LDs, we performed subcellular fractionation studies as

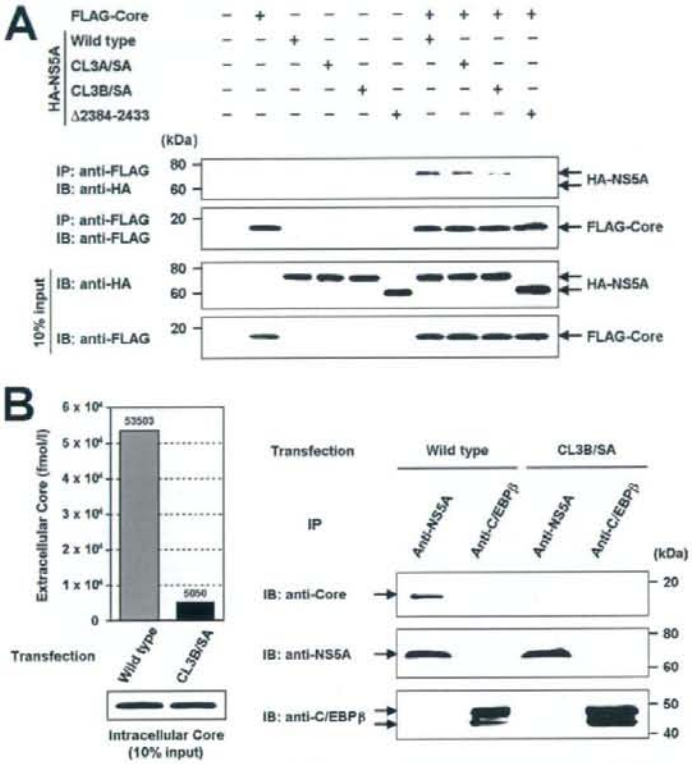

FIG. 4. aa 2428, 2430, and 2433 are essential for the interaction between NS5A and the core protein. (A) Effect of mutations at the NS5A C terminus on the interaction of NS5A with the core protein. N-terminally FLAG-tagged core protein and N-terminally HA-tagged NS5A carrying defined mutations were coexpressed in Huh-7 cells and immunoprecipitated with anti-FLAG antibody. The resulting precipitates were examined by immunoblotting using anti-HA or FLAG antibody. One-tenth of the cell lysates used in IP is shown as the 10% input. (B) Interaction between NS5A and the core protein in HCV-replicating cells. Huh-7 cells were lysed 72 h after transfection of the in vitro transcript of the HCV genome (wild type or CL3B/SA) and were immunoprecipitated with anti-NS5A antibody or anti-C/EBPβ antibody as a negative control. The resulting precipitates were examined by immunoblotting using anti-core protein, NS5A, or C/EBPβ antibody. One-tenth of cell lysates used in IP was immunoblotted with anti-core protein antibody (10% input). Cell culture supernatants harvested from transfected cells were analyzed by a core protein ELISA in parallel. IB, immunoblotting.

described in Materials and Methods. The iodixanol gradient was collected from the top to the bottom into 12 fractions (fractions 1 to 12). As shown in Fig. 7C, an ER marker, calnexin, was found in fractions 7 to 12 and was localized primarily in fractions 11 and 12. In contrast, ADRP, a cellular marker for LDs, was mainly observed in fractions 4 to 7. These two markers were equally distributed among cells analyzed (data not shown). The distribution of the wild-type NS5A was found in fractions 4 to 7, which was parallel to the fractionation profile of ADRP. The CL3B/SA-mutated NS5A was more broadly distributed and was also observed in heavier fractions than the wild-type NS5A, which was analogous to distribution of NS5A expressed in JFH1/4-1 cells bearing subgenomic replicons. The core protein in cells expressing the JFH-1 wild type, the CL3B/SA mutant, and in Huh/c-p7 cells that express JFH-1 structural proteins was distributed in a similar fashion, indicating that the distribution of core protein is not affected by NS5A mutation. The fractionation profile of the core protein, with a peak in fraction 4 or 5, was similar to that of the wild-type NS5A or ADRP but not to that of the CL3B/SA-mutated NS5A or calnexin, suggesting that core protein interacts with the wild-type NS5A in LD fractions, which is consistent with previous reports (33, 44, 45).

NS5A-core protein interaction is important for association of the core protein with the viral genomic RNA. To further address our hypothesis regarding involvement of NS5A in recruiting viral RNA to nucleocapsid formation, we analyzed the association of the core protein with HCV RNA in wild-type- or CL3B/SA-expressing cells by IP-RT-PCR (Fig. 8). Both cell lysates were immunoprecipitated with an anti-core protein antibody or a negative control, mouse IgG. Total RNA prepared from each immunoprecipitate was subjected to RT-PCR in order to detect HCV RNA. The amounts of immunoprecipitated core protein (Fig. 8, lower panel) as well as the expression of HCV RNA (Fig. 8, upper panels, Input) were comparable in both cells. In cells expressing the wild-type JFH-1 genome, the viral RNAs covering the 5′ terminal 2.2-kb as well as the 3′ terminal 2.2-kb regions were detected in immunopre-

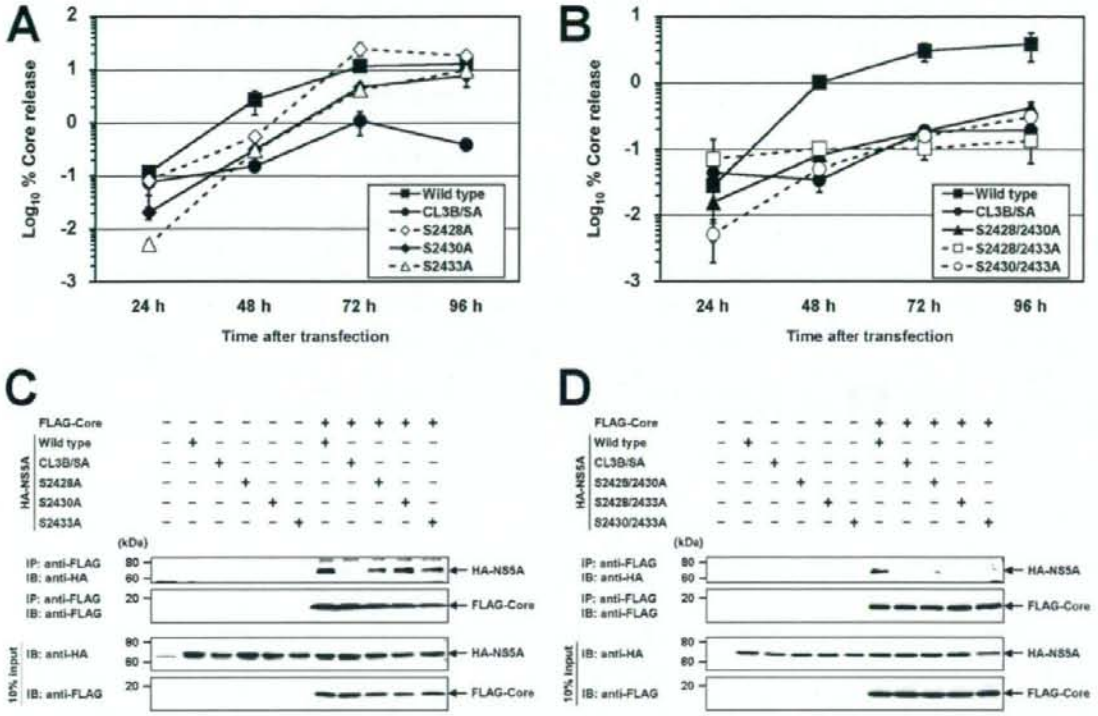

FIG. 5. Determination of critical amino acids responsible for virus production and the interaction of NS5A with the core protein. (A and B) Effect of single or double serine-to-alanine substitutions on virus production. After transfection of in vitro transcripts of the HCV genomes specified in the inset into Huh-7 cells, the cells and culture supernatants were harvested at the time points given, and the amounts of the core protein were determined by core protein-specific ELISA. Percent core protein release (vertical axis) indicates the percentage of released core protein in relation to total core protein (the sum of intra- and extracellular core protein) calculated for each time point. Mean values and standard deviations for at least triplicate experiments are shown. (C and D) Effect of single or double serine-to-alanine substitutions on the interaction between NS5A and the core protein. N-terminally FLAG-tagged core protein and N-terminally HA-tagged NS5A carrying defined mutations were coexpressed in Huh-7 cells and immunoprecipitated with anti-FLAG antibody. The resulting precipitates were examined by immunoblotting using anti-HA or FLAG antibody. One-tenth of the cell lysates used in IP is shown as the 10% input. IB, immunoblotting.

cipitates obtained with the anti-core protein antibody but not with the mouse IgG. In contrast, in cells expressing the CL3B/SA genome, HCV RNA was not detected in the immunoprecipitates with either antibody. These results demonstrate that HCV RNA associates with the core protein in cells where NS5A interacts with core protein (JFH-1 wild type) but not in cells where their interaction is impaired (CL3B/SA).

DISCUSSION

In the present study, we demonstrated the involvement of NS5A in the production of HCV particles via the interaction of NS5A with the core protein and identified its C-terminal serine cluster 3-B (aa 2428, 2430, and 2433), which is implicated in basal phosphorylation, as a key element for the interaction of NS5A with the core protein and for infectious virus production. Serine-to-alanine substitutions at the cluster, which have no impact on viral RNA replication, inhibit the interaction between NS5A and the core protein, thereby indicating that there is a connection between NS5A-core protein association and virus production. Finally, CL3B mutation leads to impairment of the association of the core protein with HCV RNA and, therefore, possibly RNA encapsidation.

Several reports have indicated that viral NS proteins are involved in the virion assembly of *Flaviviridae* viruses (25, 29, 30, 33). For instance, mutations in yellow fever virus NS2A block production of infectious virus, and this perturbation can be released by a suppressor mutation in NS3 (25), while the hydrophobic residues of Kunjin virus NS2A required for virus assembly have been mapped (26). Miyanari et al. have shown that HCV core protein recruits NS proteins to the LD-associated membranes and that the NS proteins around the LDs participate in the assembly of infectious viral particles (33). Furthermore, during preparation of the current article, two studies regarding participation of NS5A in the assembly of HCV particles were published. Appel et al. have demonstrated the essential role of domain III of NS5A in the formation of infectious particles, and deletions in this domain that disrupt colocalization of NS5A and the core protein abrogate virion production (2). Tellinghuisen et al. identified a serine residue in domain III as a key determinant for viral particle production

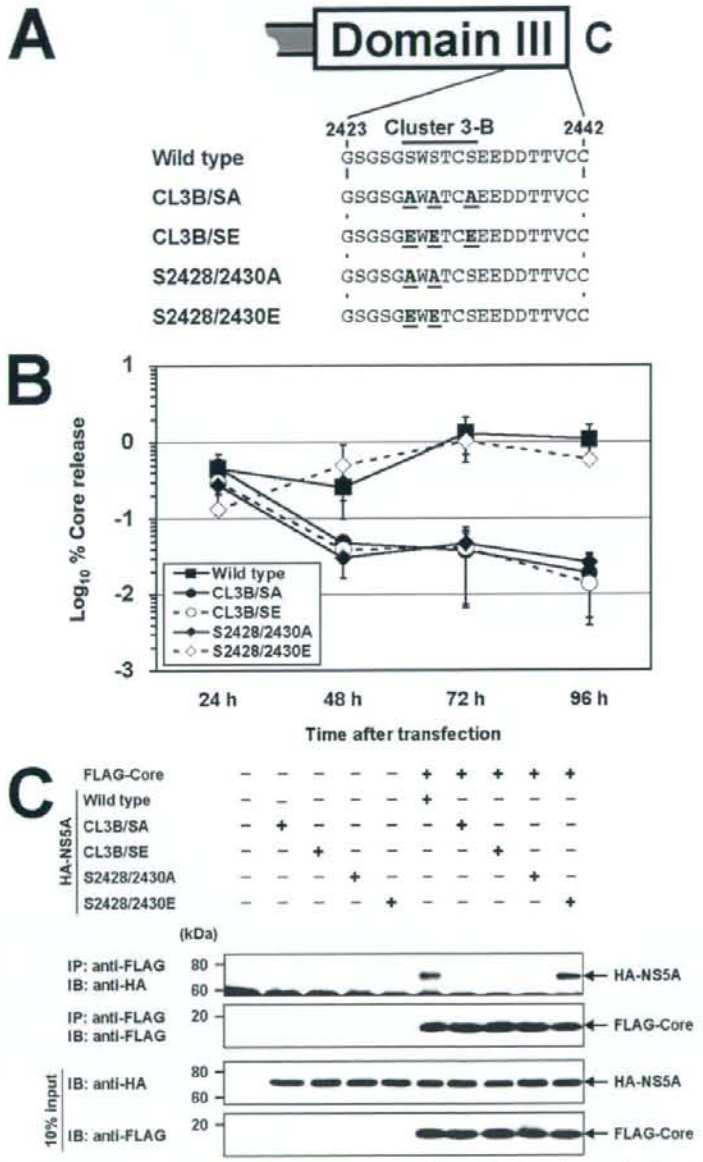

FIG. 6. Effect of glutamic acid substitutions for phosphoserines at aa 2428, 2430, and 2433 on virus production and the interaction of NS5A with the core protein. (A) Alanine or glutamic acid substitutions for serine residues at aa 2428, 2430, and 2433. The numbers indicate amino acid positions within the polyprotein of the JFH-1 isolate. The names shown on the left represent full-length HCV or N-terminally HA-tagged NS5A constructs used in this experiment. Amino acid substitutions are marked in bold and underlined. C represents the C terminus. (B) Effect of alanine or glutamic acid substitutions on virus production. After transfection of in vitro transcripts of the HCV genomes specified in the inset into Huh-7 cells, the cells and the culture supernatants were harvested at the time points given, and the amounts of core protein were determined by core protein-specific ELISA. Percent core protein release (vertical axis) indicates the percentage of released core protein in relation to total core protein (the sum of intra- and extracellular core protein) calculated for each time point. Mean values and standard deviations for at least triplicate experiments are shown. (C) Effect of alanine or glutamic acid substitutions on the interaction between NS5A and the core protein. N-terminally FLAG-tagged core protein and N-terminally HA-tagged NS5A carrying defined mutations were coexpressed in Huh-7 cells and immunoprecipitated with anti-FLAG antibody. The resulting precipitates were examined by immunoblotting (IB) using anti-HA or FLAG antibody. One-tenth of the cell lysates used in IP is as shown as the 10% input.

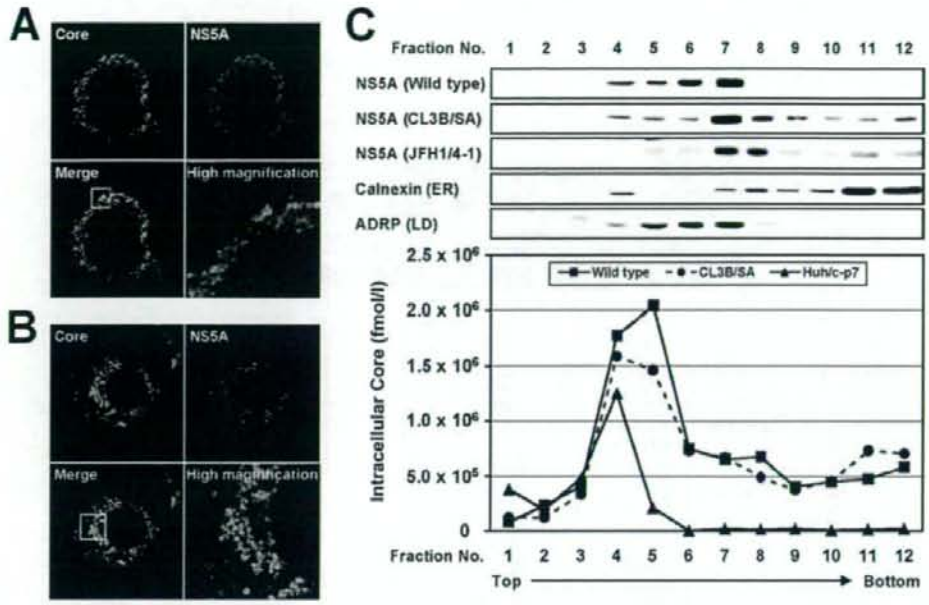

FIG. 7. Subcellular localization of NS5A and the core protein in HCV-replicating cells. Huh-7 cells were transfected with the in vitro transcript of the HCV genome, wild type (A) or CL3B/SA (B). Seventy-two hours after transfection, the cells were fixed with 4% paraformaldehyde, permeabilized with 0.3% Triton X-100, and double stained with antibodies against the core protein (green) and NS5A (red), followed by staining with an Alexa Fluor 488- or Alexa Fluor 555-conjugated antibody. High-magnification panels are enlarged images of white squares in the merge panels. (C) HCV (wild type or CL3B/SA)-replicating cells, JFH1/4-1 cells harboring a subgenomic replicon of JFH-1, or Huh/c-p7 cells stably expressing JFH-1 structural proteins were lysed by freeze-thawing, and the cell lysates were fractionated on 5 to 25% iodixanol gradients. The distributions of NS5A, calnexin (ER marker), and ADRP (LD marker) were determined by immunoblotting, and those of the core protein were examined by core protein-specific ELISA.

(50). However, the mechanism by which NS proteins participate in virus assembly or the role of the interaction between structural and NS proteins in virus life cycles has not been fully elucidated. Here, we have clearly demonstrated that HCV NS5A interacts with the core protein in coimmunoprecipitation experiments not only with coexpression of each epitope-tagged protein but also with cells expressing the viral genome; and by using immunofluorescence and subcellular fractionation analysis, we have confirmed that mutations in CL3B abolish colocalization of NS5A and the core protein, presumably around LDs. In addition, the intracellular infectivity assay and IP-RT-PCR strongly suggest that impairment of the NS5A-core protein interaction results in disruption of virus production at an early stage of virion assembly. On the basis of the present results and findings in accompanying articles, one may infer the following events: newly synthesized HCV RNAs bound to NS5A are released from the replication complex-containing membrane compartment and can be captured by the core protein via interaction with domain III of NS5A at the surface of LDs or LD-associated membranes. Consequently, the viral RNAs are encapsidated, and virion assembly proceeds in the local environment. Recruitment of newly synthesized viral RNAs to the core protein could be important for efficient nucleocapsid formation in cells, where concentrations of the viral genome and the structural proteins are typically low, and may contribute to the selection of the viral genome to be packaged. Interaction between NS5A and the core protein has been previously reported, and the NS5A region containing an interferon sensitivity determining region and the PKR-binding sequence (aa 2212 to 2330) has been mapped to that required for binding with core protein by yeast two-hybrid and in vitro pull-down assays (13). However, involvement of domain III in the NS5A-core protein interaction was not analyzed in detail, and a role for the NS5A-core protein interaction in the HCV life cycle was not examined in that study.

A growing body of evidence points to phosphorylation of NS5A as being important in controlling HCV RNA replication. Although the degree and the requirement for its hyperphosphorylation diverge between different HCV isolates, mutations that are associated with increased replicative fitness of HCV replicons frequently lead to a reduced level of NS5A hyperphosphorylation (1, 5, 36). Inhibitors of serine/threonine protein kinases that block NS5A hyperphosphorylation facilitate replication of a non-culture-adapted replicon (3, 36). One model that has been proposed suggests that NS5A hyperphosphorylation negatively regulates HCV RNA replication by disrupting the interaction between NS5A and the vesicle-associated membrane protein-associated protein subtype A, a cellular factor considered necessary for efficient RNA replication (5). However, the regulatory role of the basal phosphorylation of NS5A in the viral life cycle is poorly understood. It has been reported that the C-terminal region of NS5A (aa 2350 to 2419)